Change Detection of Hydro-Acoustic Environment for Yangtze Finless Porpoise Using Remote Sensing in Poyang Lake

Xiao Jing

March, 2008

Change Detection of Hydro-Acoustic Environment for Yangtze Finless Porpoise Using Remote Sensing in Poyang Lake

by

Xiao Jing

Thesis submitted to the International Institute for Geo-information Science and Earth Observation (The Netherlands) and the School of Resource and Environment Science (SRES) of Wuhan University (China) in partial fulfillment for the requirements for the degree of Master of Science in Geo-information Science and Earth Observation, Specialisation: Geo-information for Natural Resource and Environment Management.

Thesis Assessment Board

Prof. Dr. Ir. Alfred de Gier, Chairman (ITC)
Prof. Dr. Liu Yaolin, Dean (SRES)
, External Examiner ( )
Dr. Michael Weir, Course Director (ITC)
Prof. Dr. Ai Tinghua, Supervisor (SRES)

Supervisors: Dr. Jan de Leeuw (ITC), Prof. Dr. Ai Tinghua (SRES), Prof. Dr. Wang Ding (CAS)

INTERNATIONAL INSTITUTE FOR GEO-INFORMATION SCIENCE AND EARTH OBSERVATION
ENSCHEDE, THE NETHERLANDS
SCHOOL OF RESOURCES AND ENVIRONMENTAL SCIENCE (SRES)
WUHAN UNIVERSITY, CHINA

Disclaimer

This document describes work undertaken as part of a programme of study at the International Institute for Geo-Information Science and Earth Observation. All views and opinions expressed therein remain the sole responsibility of the author, and do not necessarily represent those of the institute

Abstract

Recently, the population of Yangtze finless porpoise has been declining. Dredging in Poyang Lake might possibly influence the acoustic environment of the porpoise which relies on echolocation for communication and detection of their prey. A better insight in the spatial distribution of dredging related noise would be useful to assess possible impacts. Traditional in situ measurements of hydro acoustic pollution are however costly to carry out. The aim of this study was to detect change of the hydro-acoustic environment induced by noise from dredging platforms and vessels transporting sand.

In situ measurement of the SPL of platforms and vessels and remotely sensed localization of this infrastructure was used to develop a model predicting SPL. The near-infrared bands of ASTER were used to classify active platforms, mobile vessels and other dredging infrastructures. The time interval between the stereo pair (band 3N and 3B) was used to separate mobile vessels from static infrastructure, while the size of objects was used to distinguish active platforms composed of a platform with associated vessels from smaller inactive platforms and immobile vessels.

Remotely sensing based noise maps of 2000, 2005 and 2006 revealed an increase in broad bandwidth noise which corresponded to the levels recorded in situ in 2007. The high frequency noise level measured in 2007 differed considerably from the remote sensing based sound predictions. Spectral overlap between the noise generated by the dredging platform and the sound used by porpoise suggests that dredging might possibly influence the echolocation of porpoise. The highly increased SPL in the northern part of Poyang Lake might disturb the behavior of the porpoise, and might isolate the population in Poyang Lake from others. Since there is a high possibility of threatening the survival of the Yangtze finless porpoise by dredging, some measures should be taken to eliminate or alleviate the impacts, such as relocating the dredging activities or replacing the noisy by more silent dredging and transport equipment.

Key Words: acoustic environment; ship detection; ASTER image; stereo pair; sound propagation model; Yangtze finless porpoise; dredging.

I dedicate this piece of work to

my family

Acknowledgements

At the time of finishing my thesis, I would like to express my sincere thanks and deepest appreciation to all the people who gave me help and support during this research.

First and foremost, I want to express my appreciation to my good friend Mr. Dong Lijun. It is him who helped me to focus on this interesting problem and started my research.

I am very grateful to Dr. Jan de Leeuw, my primary supervisor, for teaching me how to conduct a research in a scientific framework step by step. I am indebted for his close guidance, valuable comments, words of encouragement, moral support and his ever accommodating nature. I would like to extend my earnest gratitude to Prof. Ai Tinghua for the financial support and the studying environment he provided me. My sincere gratitude also goes to Prof. Wang Ding and his students for their kindness and support, especially for Dr. Li. Songhai and Mr. Dong Shouyue. Without their valuable suggestions and sharing of knowledge with me, I could not complete this research successfully. Another special word of thanks goes to my good friend Mr. Zu Yan who provided great help on the programming part of this research.

I am obliged to Mr. Wang Tiejun, Mr. Wu Guofeng and Ms. Zhao Xi for the continuous help and valuable advice from the beginning of the study. Thanks very much to Mr. Wang Tiejun for the suggestions and encouragement when I came cross problems, both in study and in my life. I would like to thank Mr. Chen Lanzhou and Mr. Liu Jianwei for their company during the field work. I also thank Dr. David Rossiter for all the statistics classes and all the praise he gave me.

I am grateful to my classmates in ITC and all my clustermates in Wuhan University for being helpful and kind to me. Thank you very much for making both places very joyful for working in. Studying with you has been interesting.. Thanks to all my international and Chinese friends for sharing all my happiness and sadness.

With gratitude I remember my parents. Thank you for providing me this precious chance to study in ITC and opening my eyes to the world.

Table of Contents

List of Figures

List of Tables and Appendices

Abbreviations

ASTER	Advanced Spaceborne Thermal Emission and Reflection Radiometer
BW	Bandwidth
IDW	Inverse Distance Weighting
RS	Remote Sensing
SL	Source Level
SPL	Sound Pressure Level
SAR	Synthetic Aperture Rader
VNIR	Visible and Near Infrared

1. Introduction

1.1 Background

The Yangtze is a unique river from the perspective of aquatic mammalian biodiversity while it is known to host two species of Cetaceans. Originally, the Yangtze river dolphin or Baiji (*Lipotes vexillifer*) and the Yangtze finless porpoise (*Neophocaena phocaeniodes asiaeorientalis*) (1992; Gao and Zhou 1995) inhabited the lower Yangtze, its associated lakes and tributaries. The populations of these two Cetaceans have declined dramatically in resent years. Not a single Baiji was found during a recent survey along the main channel of the Yangtze. This led to the conclusion that the Baiji might well be extinct (Zhao 2007). Moreover, the population of the Yangtze finless porpoise declined from 2700 in 1993 (Zhang, Liu et al. 1993) to around 1600 in 2007. Today 1100 porpoises live in the river, while 100 reside in Dongting lake and 400 in Poyang Lake (Yang, Xiao et al. 2000; Zhao 2007). The IUCN classified the Yangtze finless porpoise as endangered (EN c2b) in the Red List (IUCN 2007).

Riverine Cetaceans are under pressure all around the world. The populations of many species are declining with several approaching extinction, such as the Indus River dolphin (*Platanista minor*) in Pakistan (Braulik 2006), the vaquita (*Phocena sinus*) in the northern Gulf of California (Rojas-Bracho, Reeves et al. 2006), the Susu (*Platanista gangetica*) in Asia (Smith, Sinha et al. 1994), and the Amazon River dolphins (*Inia geoffrensis*) (Martin and F da Silva 2004). A number of causes are considered responsible for this decline, including water construction of dams and irrigation barrages, pollution by untreated urban sewage, agricultural runoff and industrial effluent, incidental killing by fishing nets, reduced abundance of prey due to overfishing and habitat degradation (Ligon, Dietrich et al. 1995; Reeves and Chaudhry 1998; Reeves, Smith et al. 2000; Braulik 2006). Electric fishing, underwater explosion, water project development and dredging are among the factors held responsible for the decline of the two species inhabiting the Yangtze (Wang, Wang et al. 2006). Further increase in utilization of the Yangtze and its associated lakes may lead to a further decline of the population of the Yangtze finless porpoise. Insight in the factors causing the decline of the porpoise would be required to avoid the Yangtze finless porpoise going the same way with Baiji.

Dredging is a factor which so far escaped research. It is relevant to consider this more closely as Poyang Lake accommodates one quarter of the total porpoise population and intensive dredging started in Poyang Lake since 2001 following a ban on dredging in the Yangtze in 1998 (Zhong and Chen 2005). Stimulated by profit, the number of dredging vessels increased rapidly (Wu, de Leeuw et al. 2007). The dredging activities concentrate in the channel in the northern part of Poyang Lake which has high densities of porpoise (Yang, Xiao et al. 2000). Northern part of the lake also allows the porpoise to move between the Yangtze and Poyang Lake, and might thus be of biological importance while allowing the Poyang sub-population to remain in contact with the subpopulation of the Yangtze.

Dredging may have a number of impacts on the porpoise. Dredging induced increased suspended sediment concentration (Wu, de Leeuw et al. 2007) may destroy the habitat of fishes (Zhong and Chen 2005), which are the food of the porpoise. The noise generated by dredging may cause problems as the porpoise relies on echo-sounding for their orientation, prey location and communication (Au 1993). It is thus suggestible that the noise generated by dredging might impede porpoise perception of their environment. Noise has also been reported to cause avoidance, hearing threshold shift and debilitation in cetaceans (Kastak, Schusterman et al. 1999; Erbe 2002; Wursig and Greene 2002; Parsons and Dolman 2003; Kastelein, van der Heul et al. 2006). This review thus indicates that a better insight in how dredging affected the aquatic acoustic environment might help to understand the impacts of the changes in hydro-acoustic environment on porpoise.

Studies on the impacts of noise on cetaceans are mostly from the marine environment. These include studies on the behavioral or physical discomfort caused by specific frequency distribution and energy (Richardson, Greene et al. 1995; Kastak, Schusterman et al. 1999; Kastelein, Verboom et al. 2005; Kastelein, van der Heul et al. 2006), Other studies focus on zones of impacts on cetaceans, such as zone of audibility, zone of masking and zone of disturbance based on the responses (Erbe and Farmer 1998; Erbe, King et al. 1999; Erbe and Farmer 2000; Erbe and Farmer 2000; Erbe 2002).

So far, little attention has been paid to the question whether it would be possible to map and monitor change in the underwater acoustic environment of marine mammals. Mapping the hydro-acoustic environment is typically done while recording noise levels in the field using hydrophones. The costs of such field based methods limit their application over wider areas. Sound propagation models (Brekhovskikh and Lysanov 1982; Vador 2000; Vador 2001; Simmonds, Dolman et al. 2003; Vador 2005; Vador 2006) allow predicting noise levels when the source of the noise is known. Such methods have been applied to model noise distribution from static sources such as icebreakers (Erbe and Farmer 2000). So far no attempt has been made to model the distribution of noise generated by mobile sources, as is the case with dredging infrastructures.

Remote sensing (RS) offers so far unexplored possibilities to localize the distribution of vessels as a source of noise. McDonnel's paper (1978) resulted in the development of two main RS techniques for ship detection, based on the optical RS (McDonnel and Lewis 1978; Burgess 1993; Tunaley 2004) or on the Synthetic Aperture Rader (SAR) images (Liu, Fang et al. 2003; Courmontagne 2005; Tello, Lopez-Martinez et al. 2006; Tello, Lopez-Martinez et al. 2006). Recently, Wu (2007) tested a method on detecting dredging infrastructures from turbid water which is similar with the situation in this research, using the infrared bands of Landsat TM image.

Vessel detection alone does however not suffice to localize noise generating dredging infrastructure as some platforms and vessels produce noise while others do not. So far no methods have been proposed to classify dredging infrastructure according to the noise level. Besides, most underwater sound propagation models have been implemented in deep water marine environments (Bowlin, Spiesberger et al. 1992; Vador 2000; Vador 2001; Vador 2005; Zhou, Zhang et al. 2007).

Developing a noise propagation model for a shallow freshwater environment is another challenge taken up in this study.

1.2 Research Objectives

1.2.1 General Objective

This research aims to detect change of the acoustic environment in Poyang Lake based on remote sensing derived localization of dredging infrastructures (dredging platforms & vessels) in order to assess the possible impacts of noise from dredging activities on the Yangtze finless porpoise.

1.2.2 Specific Objectives

- To measure the noise of dredging platforms and vessels and investigate whether this overlaps with the echolocation used by the Yangtze finless porpoise;
- To investigate whether remote sensing allows to localize and distinguish dredging platforms and mobile vessels and immobile infrastructures;
- To predict the hydro-acoustic environment of Poyang Lake and analyze the change in recent years;
- To assess the possible impacts of the changed acoustic environment on Yangtze finless porpoise.

1.3 Research Questions

- What is the energy and frequency of the noise generated by platforms and moving vessels?
- Does dredging noise interfere with acoustic range used by the Yangtze finless porpoise?
- Is it possible to detect and distinguish dredging infrastructures from satellite imagery?
- How can propagation of noise in Poyang Lake be modeled?
- Has the noise distribution in Poyang Lake changed since 2000?
- In what ways might the observed change of the acoustic environment influence the Yangtze finless porpoise?

1.4 Research Approach

In order to map the acoustic environment based on the locations of dredging infrastructures derived from remote sensing imagery, vessel detection and distinguishing, sound propagation model and the spectrum of the noise sources are necessary (Fig. 1).

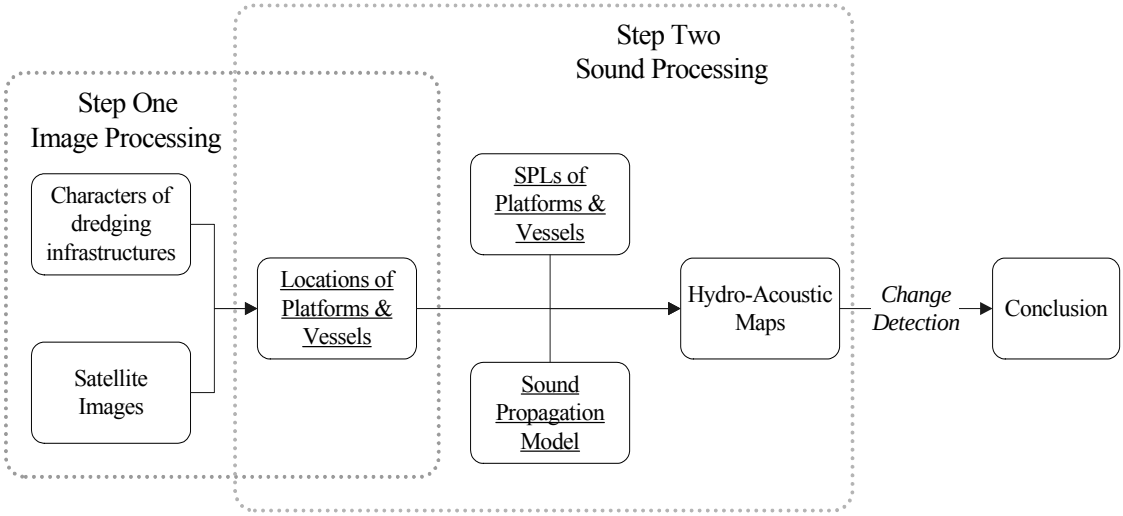

Fig. 1 -- Framework of the research

The whole research is mainly composed of two steps, image processing step followed by sound processing step. In the image processing step, the characteristics of the infrastructures which need to be extracted from the images are studied, such as the differences in size and behavior. Based on those characteristics, suitable imagery can be chosen, following the detecting and distinguishing of the dredging platforms and moving vessels. In step 2, with the location of different dredging infrastructures, the recorded noise samples of platforms and moving vessels, and the sound propagation model are used together to generated the hydro-acoustic maps. Finally, with the maps of recent years, the change of the acoustic environment of Poyang Lake can be detected.

1.5 Basic Knowledge of Underwater Noise

1.5.1 Sound Pressure Level (SPL)

This section summarizes (Simmonds, Dolman et al. 2003):
The most commonly used term for describing the loudness of sound is sound pressure level (SPL) expressed in decibel (dB):

$$SPL = 20\log_{10}(\frac{p}{p_{ref}}) \quad dB \cdot re \cdot 1\mu Pa$$

Where p (expressed in micropascals, μPa) is the measured pressure defined as the sound force per unit area, and p_{ref} is the reference pressure which equals 1 and 20 μPa underwater and in air respectively. The reference pressures under water and in air are defined according to the abilities of terrestrial and marine mammals to detect the change of the loudness of the sound. So, a direct comparison of SPL measured in air and under water cannot be made. But after adjustment of the difference in pressure reference levels, and the differences in acoustic impedance, it might be assumed that an equivalent SPL underwater of a measure one in air could be achieved by adding 62 dB. However, this may be a risky comparison because the mechanisms leading to damage in the ear underwater maybe significantly different from that in air.

1.5.2 Ambient Noise Measurement

This section summarizes (Chen, Zeng et al. 2005):
The intensity of noise is normally expressed as the average sound power over a certain bandwidth (BW). The typical unit for noise measurement is sound power in 1Hz band (Pa^2 / Hz), named noise spectrum level or noise power spectral density.

$$10\log_{10}(p^2 / BW) = 20\log_{10}(p / p_0) \ -10\log_{10}(BW / 1)$$

BW is defined as the upper “cutoff frequency” minus the lower “cutoff frequency”. The reference for BW is 1 Hz. The pressure reference (p_0) in water is $1\mu Pa$.

2. Methods and Materials

2.1 Study Area

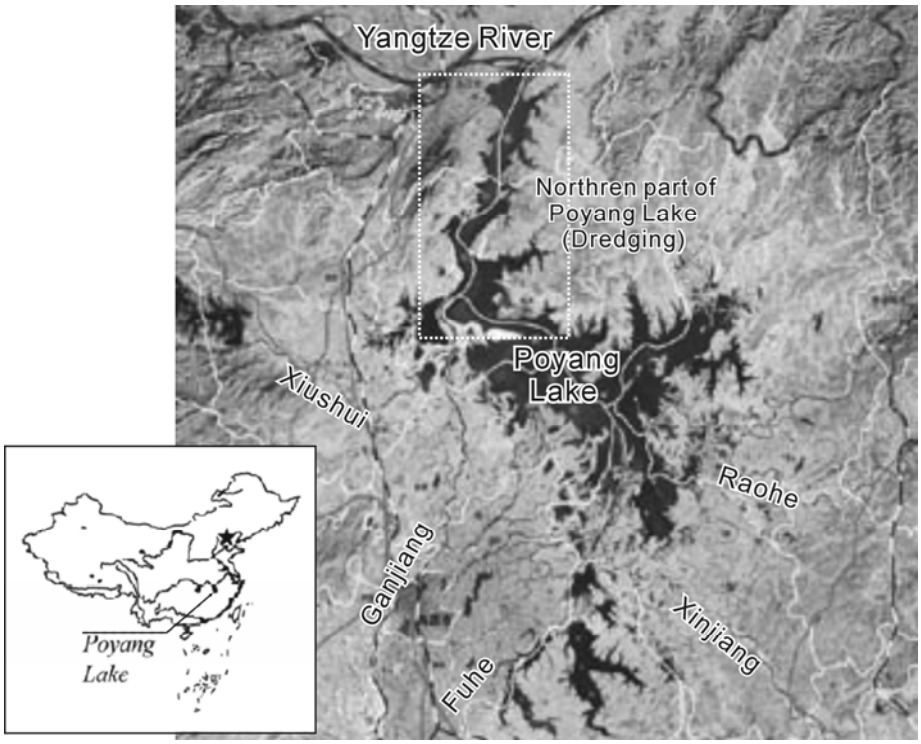

Fig. 2 -- Location of Poyang Lake

Poyang Lake is the largest freshwater lake in China. It (28° 22′ - 29° 45′ N, 115° 47′- 116° 45′ E) locates in the Jiujiang City, Jiangxi Province (shown in Fig. 2). The average surface area of this lake is 3,585 km^2 (4,400 km^2 during rainy season, 1000 km^2 during dry season), with average water depth of 8.4 m (max depth 25.1m) (http://en.wikipedia.org/wiki/Poyang). It is mainly fed by the Ganjiang and Xiushui, and connects to Yangtze River through a channel in the northern part.

Furthermore, Poyang Lake is one of the main habitats of the Yangtze finless porpoise now. The number of the finless porpoise living in it is around 400, changing with the seasons, water depth and the fish resources (Xiao and Zhang 2002). One finless porpoise reserve has also been established within Poyang Lake.

However, since 2000 when dredging activities began in Poyang Lake, the number of dredging vessels increased from zero in 2000 to about 400 in 2005 (Wu, de Leeuw et al. 2007). It is assumed that the acoustic environment has been changed significantly by the noise generated from dredging activities. The distribution of dredging activities is uneven, most of which concentrate in the northern part of Poyang Lake, whereas there is little disturbance from it in the southern part of the lake.

2.2 Image Data Selection

Tab. 1 -- Used images and their usage

DATA	PURPOSE	DATES
ASTER Images	Detecting and distinguishing the distribution of dredging platforms and moving vessels	22/08/2000 03/07/2005 06/20/2006

All the available ASTER Images of Poyang Lake except winter time from 2000 have been searched from *Earth Observing System Date Gateway* of NASA. The year of 2000 was the last year before dredging was introduced to Poyang Lake. The image of 2000 is used to show the conditions prior to the introduction of dredging. It is supposed that there is almost no boat shown on the image of 2000, except for some small fishing boats.

Winter time is the dry season for Poyang Lake. Water begins to fade from October every year until March the next year. During the dry season, less than one quarter of the lake area in rainy season is left, leaving the main channel for transportation [Fig. 3], when most of the dredging vessels are constrained within the channel. So in order to do the comparison of the acoustic environment between different years, only the images in the rainy season are chosen when all the dredging platforms distribute in the wide range of the lake.

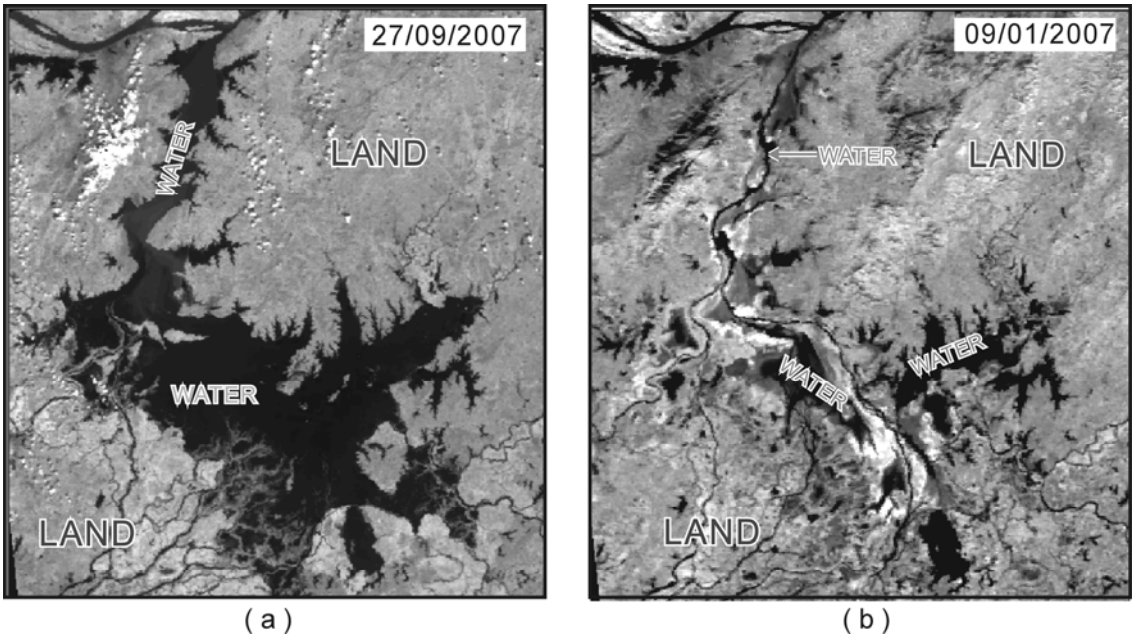

Fig. 3 -- MODIS images of Poyang Lake in rainy season and dry season. (a) shows the water area in rainy season; (b) shows the water area in dry season

For the reason that the images in 2001, 2002, 2003 and 2007 are all have too much cloud to be used for the analysis, and the only available image in 2004 is in the dry season, the three images in 2000, 2005 and 2006 are chosen for this study.

2.3 Field Data Collection

2.3.1 Needed Field Data

Table 2 lists the data collected in the field and the intended purpose for which these were to be used.

Tab. 2 -- Description of data collection in the field and their usage

DATA	PURPOSE
Sizes of dredging platforms and vessels	Foundation of distinguishing them
Noise level of dredging platforms and vessels	SPL from noise source – SL
Sample Points of noise level of the whole lake	Presenting current situation

- The different sizes of the two dredging infrastructures, their distribution patterns, and different behaviors are studied in the field. The recognizing of them on satellite image is based on these three parameters.

- The SPL of the noise generated from the dredging platforms and moving vessels are recorded to calculate the source level (SL) of different dredging infrastructures.

- Sample points of the noise SPL are measured all over the whole Poyang Lake, both in the northern part (where the dredging activities are) and southern part (where there is almost no dredging) of the lake. Those SPL are used to show the acoustic environment of Poyang Lake in the rainy season 2007.

2.3.2 Noise Data Collection

From 25th to 27th September 2007, the recordings of noise of dredging infrastructures and at samples points were made over the whole Poyang Lake. The whole investigation was carried out on small boats, starting from Hukou, passing by Xingzi, Duchang, and finally reaching Poyang. The wind over the lake decreased from 25th to 27th.

The aim of this study was to investigate noise levels relevant for the assessment of the possible impact of dredging induced noise on the finless porpoise. Restricted noise bandwidths might interfere with the echolocation while broader spectrum noise is known to disturb cetaceans. The clicks used for echolocation by the finless porpoise range from 87 to 145 kHz, with an average of 125 ± 6.92 kHz, (Li, Wang et al. 2005), which corresponds to their range of high-sensitivity hearing of 45 to 139 kHz (Popov, Supin et al. 2005). Richardson and Green (1995) reported that continuous broadband noise levels of 120 dB *re* 1 μPa lead to disturbance in cetaceans. Therefore, noises of two bandwidth ranges were chosen to be recorded. The first chosen range was

the broadband noise ranging from 0.01 to 147 kHz, the second a narrow band noise range (10-147 kHz) corresponding to the range used for echolocation. Because of the stochastic nature of the noise and part of the noise comes from the transporting noise of the dredging vessels which only comes when a vessel is passing by, each noise recording lasted for at least 5 minutes, that was least 10 minutes at each sample point. During the recording, the engine of the boat used by us was switched off to make sure that no extra noise was introduced into the recording.

The underwater noise recordings were made with a hydrophone (OKI ST1020，Oki Electric Co. Ltd.，Japan) at 1 meter water depth. The sensitivity of the hydrophone was -180 dB *re*: 1 V/ μPa +3/-12 dB, up to 150 kHz. The sensitivity declined with the increase of the frequency from 100 to 150 kHz, and the sensitivity is approximately -180 dB *re*: 1 V/ μPa +5 dB (Li, Wang et al. 2005). The underwater sound level meter (OKI SW1020) and a digital data recorder (SONY PCHB244) were used to record the signals up to 147 kHz. The frequency response of the recorder is from 10 Hz to 147 kHz ($\pm$ 3 dB) (Akamatsu, Wang et al. 1998). During the collection of the SPL at sample points, a GPS was used for navigation.

The hydrophone was used to record the sound level of dredging platforms and vessels at several random points throughout the lake. The sound level of dredging platforms was recorded while towing the hydrophone by the side of a platform. Measurements of sound levels of vessels were more problematic because it was not allowed to tow the hydrophone from moving vessels. We thus recorded the sound level of vessels while they were passing by and measuring the distance between our boat and the vessels using an adjustable ranging telescope. The sound generated by the vessels was recorded for merely one minute.

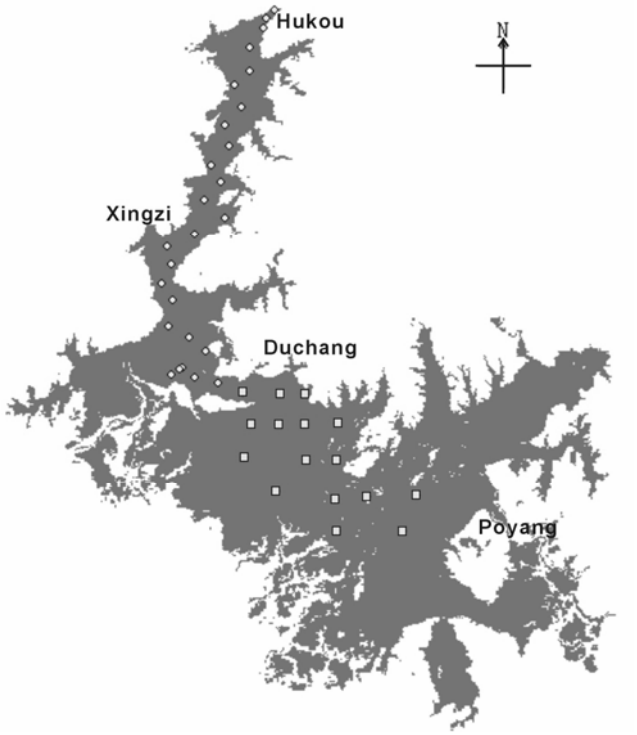

Fig. 4 -- Distribution of sample points. Circles indicate the sample points in the northern part; rectangles indicate the sample points in the southern part

Noise levels throughout the lake were sampled at forty-two points located according to a stratified regular sampling design [Fig. 4]. A higher density of sampling points was designed in the north of the lake because dredging activities concentrating there were expected to cause a higher spatial variability in noise level than in the southern part. Areas along the edge of the main body of the lake were avoided because those areas were covered by fishing nets preventing records by hydrophone. Altogether twenty-six points were sampled in the north and sixteen in the south. The distribution of the sample points in the northern part of Poyang Lake were mainly designed locating by the two sides of the main channel. Some points were added in when there was no sample point in a large area. The distance between two sample points was around 3 to 4 km, but changes were made according to the geometry of the lake. Considering the navigation of the boat, the track formed by the sample points was "Z" shape. The sample points in the main body of Poyang Lake located on the corner of a square grid, with the grid size of 5 km (3 sample points missing).

2.4 Satellite Image Processing

The unique feature of the Advanced Spaceborne Thermal Emission and Reflection Radiometer (ASTER) is the stereo pair of the near-infrared band, a nadir image (3N) and its corresponding back-looking image (3B) 55 s later (Matthews 2005). Although the stereo pair is originally designed for use in land application, it also provides a possibility of detecting moving vessels, whose locations will change on the 3B image compared with the 3N image due to the displacement during the time interval of the two images. According to Wu (Wu, de Leeuw et al. 2007), the infrared bands are good at extracting vessels from turbid water, because they can eliminate the impacts of high reflection of the sand in the water. Another advantage of the stereo pair of ASTER is the relatively high resolution of 15 meters, capable of distinguishing vessel groups from single vessel. One example is shown in Fig. 5.

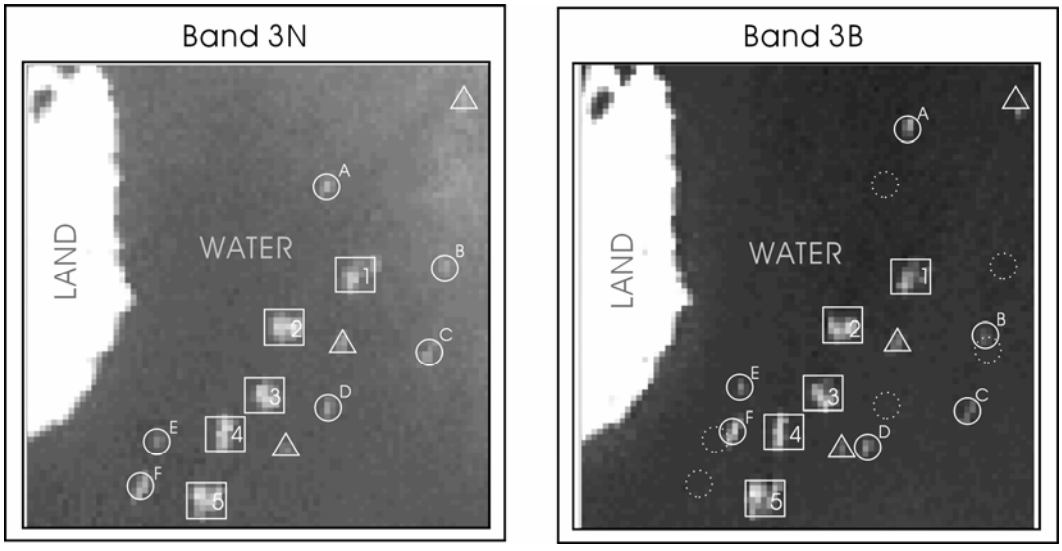

Fig. 5 -- The light objects in the water area are dredging infrastructures. Objects in the circles are moving vessels; big static objects in the squares are dredging platforms; small static objects in the triangle are immobile infrastructures

Only 4 images during the rainy reason from 2000 to 2007 are available, one in 2000, one in 2005 and two in 2006. The image in June 2006, rather than in April 2006, is chosen because it is closer with the months of images in 2000 and 2005 and the date of the field work.

The satellite image processing is composed of geometric correction and classification. An unsupervised classification is implemented to extract all the dredging infrastructures from the turbid water. After that, a manually separation of the dredging platforms, moving vessels and other infrastructures are carried out under three criteria (size difference of the two dredging infrastructures, their distribution patterns and different behaviors).

2.4.1 Geometric Correction of Images

Because of the large extent of study area, the whole area had to be separated into two portions (northern part and southern part) for the geometric correction in order to reach the acceptable precision (shown in Fig. 6).

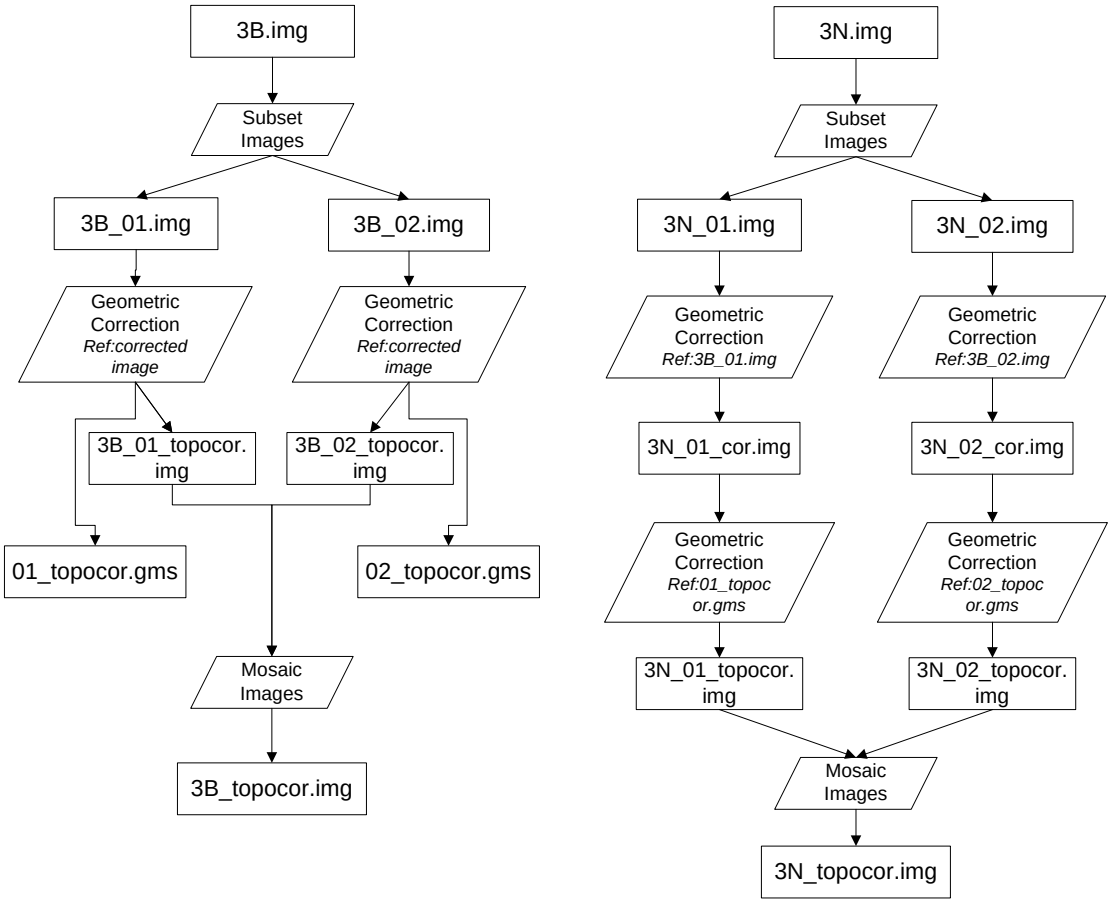

Fig. 6 -- Geometric correction of single image

Both the 3N and 3B band images were divided into two sub-images (*_01.img, *_02.img) from

the middle before the geometric correction. During the correction, each part of the 3N band was firstly corrected referencing the counterpart of the 3B band using a third order polynomial, in order to guarantee the preciseness of the relative position. The error was within one pixel in the lake area after this correction.

Then, each part of both the 3B and 3N bands were corrected referencing a geo-corrected image using the same third order polynomial model (*.gms). The corrected sub-images were combined together (mosaic images) using an average function at the end.

2.4.2 Extraction of Dredging Infrastructures

For the reason that most of the boats except for dredging infrastructures were very small as discovered in the field work (less than one pixel on ASTER), it can be assumed that all the visible objects in the Poyang Lake belong to dredging activities. In this step, all the vessels in the lake area were extracted from the turbid water [Fig. 7].

1) Subset image. Before the process, the lake area excluding all land area was subset from the whole image under the consideration that the reflectance of land is similar with the reflectance of dredging infrastructures in the near-infrared band. The subset area [Fig. 7(b)] did not contain any land or some part of water area where there is no vessel in that area.

2) Unsupervised classification. Unsupervised classification was implemented to extract all the vessels from water. After some experiment, the 4-classes classification was the best in this case. The lightest class was mostly consisted by dredging infrastructures and contained most area of one object. The second and third lightest class may be either the dark part of the infrastructures or the turbid water when the darkest class is only water [Fig. 7(d)].

3) Raster to polygon. The classified image was converted to polygon according to class values in ArcGIS, left only the polygons in the lightest class. After conversion, the polygon map was compared with the original image to wipe off some of the polygons which were not infrastructures judged by eyes, such as clouds or turbid water, leaving only the polygons of dredging infrastructures [Fig. 7 (e) (f)].

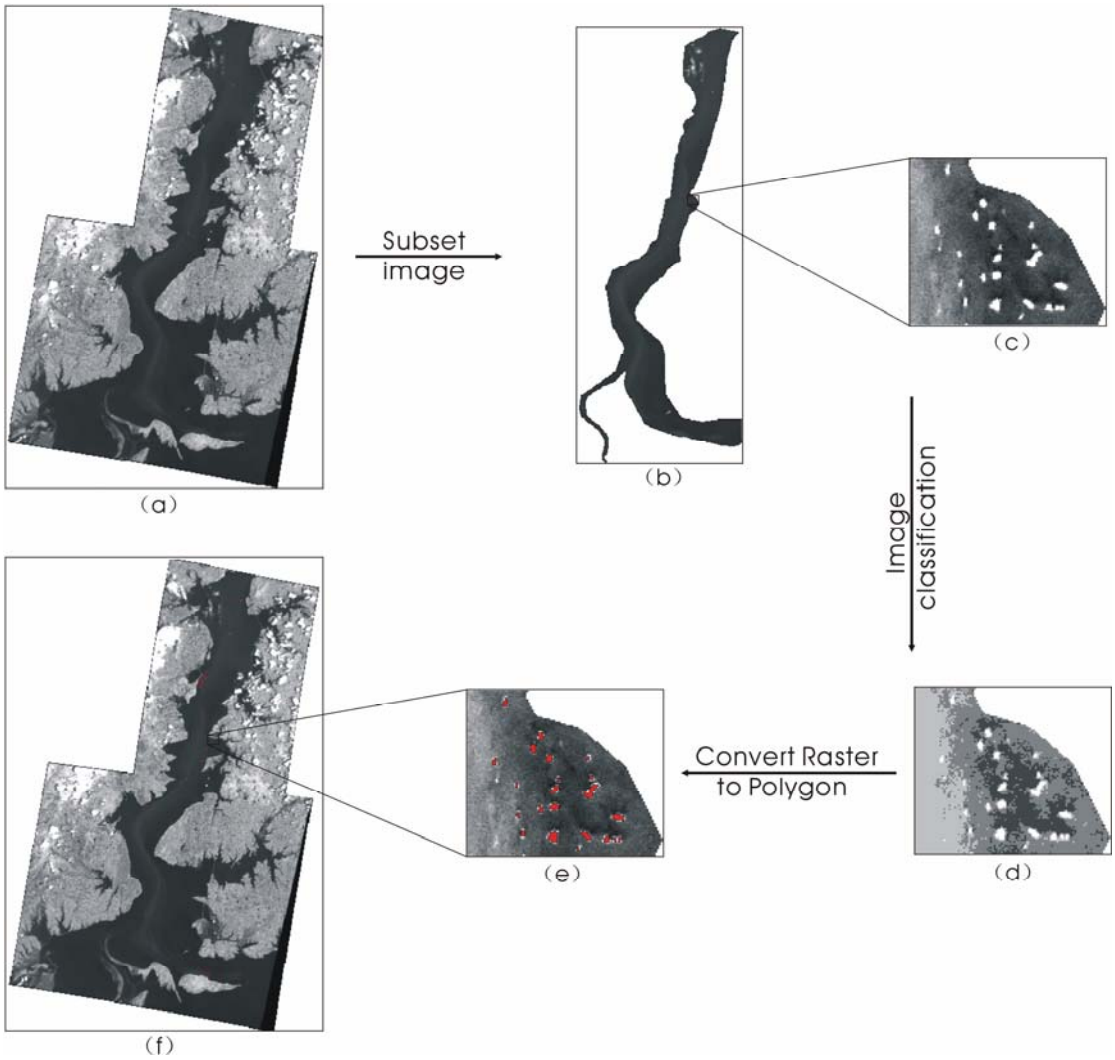

Fig. 7 -- Extraction of dredging infrastructures. (a)is the original image; (b)is the lake area; (c)is the zoomed area; (d)is the classified image; (e)shows the polygons of dredging infrastructures; (f)shows the polygons of extracted dredging infrastructures

2.4.3 Remotely Sensed Classification of Dredging Infrastructures

For the present research, noise generated from silent dredging infrastructure needed to be distinguished [Fig. 8]. During field visit it was noted that part of the boats and dredging platforms were not active and did not produce noise. The following procedures were used to separate silent dredging infrastructure from active platforms and active vessels.

Dredging platforms had according to our field observations a size of around 30m×70m, while the vessels were around 15~20m wide and 50~70m long. The difference between these was too small to allow distinction in the ASTER imagery. However, active dredging platforms were surrounded by vessels, waiting to be filled in with sand [Fig. 9]. In the ASTER image such active platforms were significantly bigger than single vessels or platforms. Based on size it was thus able to distinguish active platforms from a smaller sized category of objects including inactive platforms

and vessels. The ASTER imagery also allowed us to distinguish immobile from moving objects, the latter corresponding to active vessels which generate noise. The ASTER imagery thus enabled us to distinguish active platforms, active vessels and a remaining group of immobile and silent dredging infrastructures.

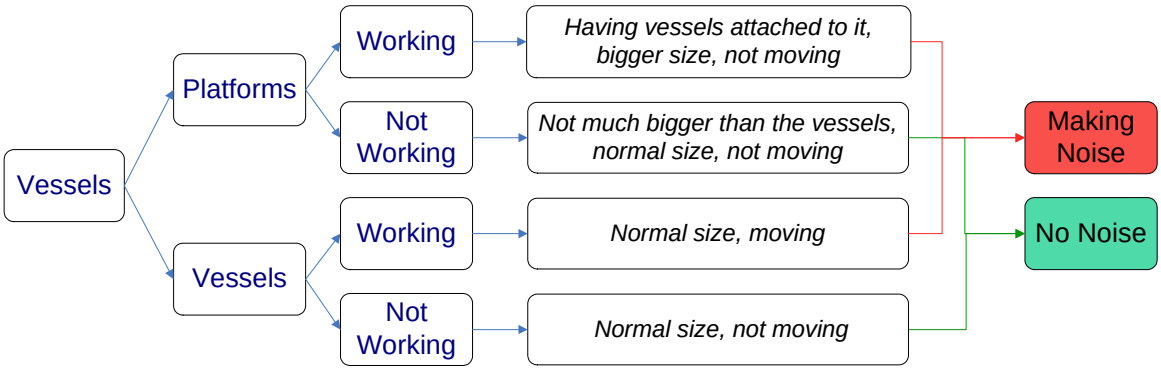

Fig. 8 -- Expert knowledge of distinguishing dredging infrastructures

Fig. 9 -- A cluster of a dredging platform. The dredging platform is second from right and the others are vessels waiting by its sides. Note the deeper position of the vessel at the right wich is being filled.

This knowledge of the difference in size and mobility between objects was used to classify dredging infrastructure into three categories according to mobility and size.

1) Mobility detection. The time difference between capturing of the 3N and 3B band of the ASTER imagery was used to discriminate moving from immobile objects. For this the 3N band was overlaid with the 3B band to visually identify mobile vessels. Sometimes the shapes of vessels differed slightly between the 3N and the corresponding 3B band, due to their different view angle. The speed of the moving vessels was around 10 km/h, which meant that vessels moved around 10 pixels (150m) in the 55 seconds which had passed between the two images. While groups of vessels were moving, their spatial arrangement remained strikingly similar because the mobile vessels moved at homogenous velocity. Objects which had the same position in the 3N and 3B were first classified static; while all other objects were

classified mobile. The location of mobile vessels in the 3N and 3B images was matched using object shape and the pattern relative to surrounding vessels. This classification is shown in Fig. 11 (a), where vessels outside the red circles were classified static. In the circles, 3 patterns can be found (pattern 1, pattern 2 and pattern 3) for moving vessels. In pattern 1, the big vessel moved from north to south; in pattern 2, the two vessels also moved from north to south; and in pattern 3, the three vessels moved from south to north.

2) Size distinction. After distinguishing mobile and static objects, static objects were next classified according to their size. Platforms had a size of 30m × 70m or 2100m^2. We considered all objects larger than 3500m^2 as an active platform because it should consist at least of a platform (30 × 70m) and one vessel (20 × 70m). An area of 3500m^2 corresponds to 15m ASTER pixels. As mixed pixels with intermediate reflectance around the main body of the vessel, might classified as water [Fig. 10], a minimum of 10 pixels was used as criterion for classification of an active dredging platform (in Fig. 11(c), the polygons in blue are the infrastructures which are more than 10 pixels big) The classification was carried out in ArcGIS.

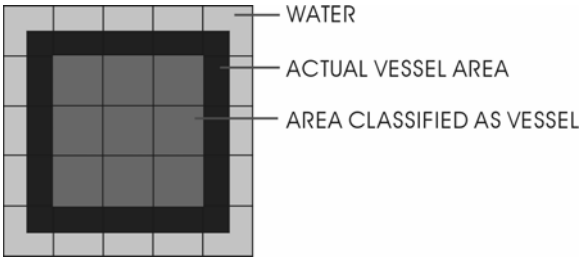

Fig. 10 -- Each square indicates one pixel on the ASTER image. Black shows the area of a vessel; deep grey area shows the pixels classified as pixels of the vessl.

3) Polygon to Point. After classification of all objects into active platforms, moving vessels and others, the polygons of other vessels were deleted as they do not produce noise. The polygons remaining were converted to points to facilitate further modeling [Fig. 11 (d)].

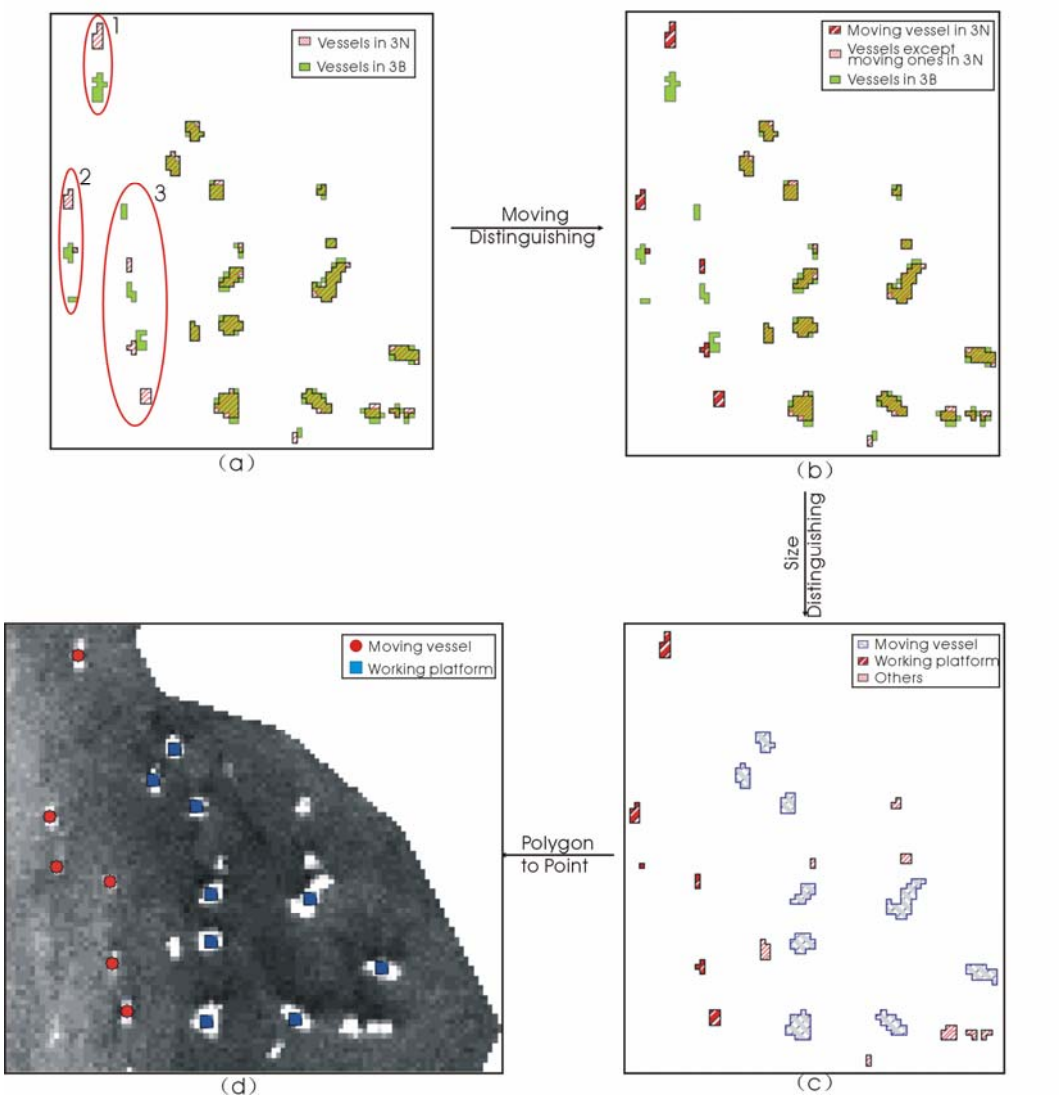

Fig. 11 -- Distinguishing of vessels.

2.5 Noise Analysis

2.5.1 Principles of Noise Analysis

1) Sound Propagation Model

The SPL decreases when the sound propagates through water. Simply the transmission loss can be estimated as the sum of the geometrical spreading loss and the water absorption loss (Simmonds, Dolman et al. 2003). So the SPL reaching the receiver can be expressed as:

$$RL = SL - (TL_{spreading} + TL_{absorption})$$ (Simmonds, Dolman et al. 2003)

RL is the SPL at the receiver;
SL is the recorded SPL of the noise source;

$TL_{spreading}$ is the sound spreading loss;

$TL_{absorption}$ is the absorption loss.

a) *Geometrical spreading loss*

There are two typical forms of spreading loss underwater. One is spherical spreading loss and the other is cylindrical spreading loss. Normally, when the water depth is less than 200m and the spreading distance is further than the water depth, the cylindrical spreading loss is suitable:

$$TL_{spreading} = 10\log_{10}\frac{R}{R_0}dB \quad R >= R_1$$ (Simmonds, Dolman et al. 2003)

R_1 is water depth (km);
R is the distance between the noise source and the receiver (m);
R_0 is reference range, usually 1m.

This formula holds when the surface and the bottom reflect all sound, which is not the case in reality. Instead the equation provided by Wuersig and Greene (2002) for spreading loss in shallow waters of less than 10m (as is the case in Poyang Lake) was used:

$$TL_{spreading} = 15\log_{10}\frac{R}{R_0}dB \quad R >= R_1$$ (Wuersig and Greene 2002)

b) *Absorption loss*

A number of experimental and theoretical works have been done on the underwater sound absorption. Some of them were conducted in the shallow coastal water (Yang 2006; Katsnel'son, Badiey et al. 2007; Zhou, Zhang et al. 2007), while others were in the deep sea (Vador 2001; Vador 2005). Some were based on the sound of low frequencies (Vador 2000), whereas others were focuses on high frequencies (Schulkin 1968; Schulkin 1969). No matter in which condition, the sound absorption is a frequency dependant loss. Based on the experiments by Schulkin (Schulkin 1968; Schulkin 1969) on the experiment at 1.5 – 25 kHz in the seawater, the water absorption model is estimated, which is also used by Vadov (2006) and published by Brekhovskikh in his book for the high frequency sound ranging from 3 kHz to 0.5 MHz (Brekhovskikh and Lysanov 1982).

$$TL_{absorption} = 8.6\times10^3[\frac{SAf_T f^2}{f_T^2+f^2}+\frac{Bf^2}{f_T}]+3(fh)^{0.5}/R_{fin} \quad dB/km$$

$$= 8.6\times10^3\times\frac{SAf_T f^2}{f_T+f^2}+8.6\times10^3\times\frac{Bf^2}{f_T}+3(fh)^{0.5}/R_{fin} \quad dB/km$$

$f_T = 21.9\times10^{[6-1520/(t+273)]}$ is the relaxation frequency (kHz);

t is the temperature（℃);
S is the salinity（‰);
f is the frequency (kHz);
A = 2.34×10^{-6};
B = 3.38×10^{-6};
H is the mean wave height (m);
R_{fin} is the length of the limiting ray cycle capture by the channel (km).

The first term ($8.6\times10^{3}\times\frac{SAf_T f^2}{f_T^2+f^2}$) is determined by the salinity, and second term ($8.6\times10^{3}\times\frac{Bf^2}{f_T}$) characterizes the sound attenuation. The third term of the formula describes the sound loss caused by wave height related surface roughness. Considering that the salinity in Poyang Lake is very low (less than 1‰) and normally there is no strong wind in the lake, so most partial of the absorption of the sound in Poyang Lake is the sound attenuation. For the reason that the temperature is changing day by day, an approximate temperature of 20℃ is chosen. As a result, the simplified formula used in this case is shown as follows:

$$TL_{absorption}=8.6\times10^{3}\times\frac{Bf^2}{f_T}=2.12\times10^{-4}\,f^2 \quad dB/km$$

When the temperature is 20℃.

2) Superposition Principle of Decibels

Normally, the sounds from two different noise sources are non-coherent, so the superposition of the sound energy is used to infer the superposition principle of decibels. The principle is shown in the formula below:

$$L_{pT}=10\log_{10}(\sum_{n=1}^{N}10^{0.1L_{pn}})$$

L_{pT} is the total SPL;
L_{pn} is the SPL by each noise source.

The principle can also be expressed using the difference of the two SPL, L_{p1} and L_{p2} (assuming that $L_{p1} > L_{p2}$)

$L_{pT}=L_{p1}+10\log_{10}(1+10^{-0.1\triangle L_p})$, when $\triangle L_p=L_{p1}-L_{p2}$

According to the formula, when the difference of two SPL is higher than 10 dB, the total SPL can be taken as the higher SPL.

2.5.2 Background Noise

During the field work, samples in the main body of Poyang Lake, where there was no dredging activities, were collected. The sound measured there can be considered as the natural sound of Poyang Lake, caused by the wind, waves and the vocalization of marine mammals and fish (Simmonds, Dolman et al. 2003). Since the measured SPL in Poyang Lake were not constant, but similar due to the various environments, the lowest SPL in each bandwidth was taken as the approximate ambient noise of the whole lake. So the ambient noise was 104 $dB{\cdot}re{\cdot}1\mu Pa$ and 92 $dB{\cdot}re{\cdot}1\mu Pa$ in the range from 0.01 kHz to 147 kHz and from 10 kHz to 147 kHz respectively.

Taking the ambient noise into consideration, another attention needs to be paid before using the measured SPL. According to the principle of sound measurement (Chen, Zeng et al. 2005), if the measured SPL is more than 10 dB higher than the ambient noise, the record reflects the real the SPL of the noise; if the difference is between 3 dB and 10 dB, the SPL of the noise should be calculated using the sound superposition principle; and if the difference is less than 3 dB, the result of the measurement is inefficient.

2.5.3 Measured Data

The SPL of the noise sources were measured at three locations, one for platform and two for moving vessels. As stated in 2.3.2, noises of two frequency ranges were measured at each location. One was broad bandwidth, from 0.01 to 147 kHz, the range of the recording machine, while the other was comparatively narrow, from 10 to 147 kHz. The recorded data is shown in the table below.

Tab. 3 -- Recorded data of noise sources

ID	TYPE	DISTANCE (m)	THRU ($dB{\cdot}re{\cdot}1\mu Pa$)	HP ($dB{\cdot}re{\cdot}1\mu Pa$)
665	Platform	15	157	114
683	One Small Vessel	20	131	*93*
669	Two Big Vessels	89	132	*92*

(THRU—SPL with the bandwidth from 0.01 kHz to 147 kHz; HP—SPL with the bandwidth from 10 kHz to 147 kHz)

As shown in the table, all the three measured data for *THRU* and the *HP* record of platform were more than 10 dB higher than the ambient noise of their corresponding bandwidth, meaning that they can be used directly in the later calculation of SL. Whereas the *HP* data were ineffective because they were less than 3 dB higher. Simply, the *HP* noise by vessels were evaluated the same

as the ambient noise, which was 92 $dB{\cdot}re{\cdot}1\mu Pa$.

1) SL of platforms

The noise was measured beside one vessel being filled with sand by a working platform. There were other four vessels waiting at the other side. The recording point is shown in Fig. 12.

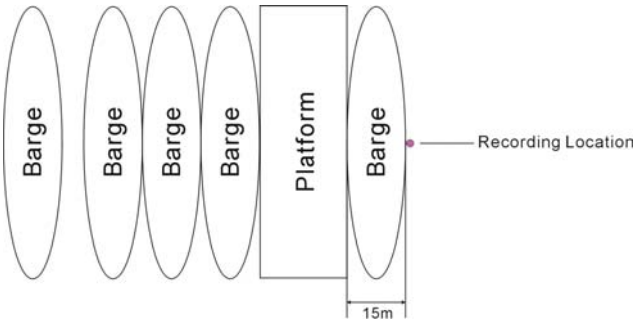

Fig. 12 -- Location of the recording point for platform.

There were at least two kinds of noises from the dredging platform, the noise from the engine and the noise from the spud during dredging. The vessels beside it might also make noise. In this case, the cluster of platform and vessels were simplified as a point and the noise of this cluster was the sum of the noises from all of them. The distance from the noise source was assumed as the distance from platform, which was the width of a vessel. Therefore, the sound loss of the noise from platform by geometrical spreading was:

$$TL_{spreading} = 15\log_{10}(15/R_0) = 17.64 \quad dB \quad (R_0 = 1)$$

Because the sound absorption loss is frequency dependant, the lowest and the highest loss of the sound in 15m were as calculated below:

$$TL_{absorption{\cdot}low} = 2.12\times10^{-4}\times(0.01)^2\times15/1000 = 3.18\times10^{-10} \quad dB$$

$$TL_{absorption{\cdot}high} = 2.12\times10^{-4}\times(147)^2\times15/1000 = 6.87\times10^{-2} \quad dB$$

Compared with the sound loss of the geometrical spreading (17.64 dB), the loss caused by absorption (less than 0.1 dB) can be ignored here.

The SL of the platform was the sum of measured SPL and the sound loss through the propagation. According to the calculation above, the SL in both bandwidths were:

$$SL_{Thru{\cdot}P} = 157 + 17.64 = 174.64 \quad dB\cdot re\cdot 1\mu Pa@1m$$

$$SL_{\mathrm{Hp{\cdot}P}} = 114 + 17.64 = 131.64 \quad dB\cdot re\cdot 1\mu Pa@1m$$

2) SL of vessels

According to the calculation, the water absorption loss of the sound in a short distance (0.4 dB within 100m) can be ignored compared with the loss by spreading, so only the geometrical spreading loss was considered in the later process.

a) SL of small vessels

The SL of the small vessel was the sum of the measured SPL and the geometrical loss through the underwater spreading:

$$SL_{Thru\cdot small} = 131 + 15\log_{10}(20/1) = 150.52 \quad dB\cdot re\cdot 1\mu Pa@1m$$

b) SL of big vessels

The measured SPL of noise was generated by two similar vessels, whose SL can be considered as the same. According to the sound superposition principle,

$$L_{pT\cdot Thru} = 10\log_{10}(10^{0.1RL_{Thru\cdot big}} + 10^{0.1RL_{Thru\cdot big}})$$

So,

$$RL_{Thru\cdot big} = L_{pT\cdot Thru} - 10\log_{10} 2 = 128.99 \quad dB\cdot re\cdot 1\mu Pa$$

Then, the SL of the big vessel for *THRU* was:

$$SL_{Thru\cdot big} = 128.99 + 15\log_{10}(89/1) = 158.23 \quad dB\cdot re\cdot 1\mu Pa@1m$$

c) Average SL of vessels

Because the sizes of the vessels cannot be recognized from ASTER image, all the vessels were considered as the same, so that the noise generated by the vessels was considered the same. Under this assumption, the average SL of small and big vessels was calculated as the common noise of each vessel. In other words, the superposition of the noise of two common vessels equals to the superposition of the small vessel and the big vessel:

$$2\times 10^{0.1SL_{Thru\cdot B}} = 10^{0.1SL_{Thru\cdot small}} + 10^{0.1SL_{Thru\cdot big}}$$

So $SL_{Thru\cdot V}$ equals to $155.90 dB\cdot re\cdot 1\mu Pa@1m$

2.5.4 Comparison of Noise and Sound of Porpoise

A spectrum diagram of the noise from the cluster of dredging platform, the ambient noise and the sound used by the Yangtze finless porpoise was made in order to determine the probability that

dredging activity has an impact on the finless porpoise. It was performed using a PC-based signal processing system, the SIGNAL/RTS^{TM} (Version 3.0). Au (1993) stated that "Ambient noise generally fluctuates unpredictably in a random fashion, or a continuous spectrum. Therefore, the amount of noise measured will depend on the bandwidth of the measurement system", the unit used for the spectra was dB re 1 μPa^2/Hz (as stated in 1.5.2). The convention of the measured noise to the spectrum obeys the formula in 1.5.2. Although it was not normal to represent the sound of finless porpoise in this unit, for the sake of comparing the spectrum level of dredging noise and the ambient noise with the sound of the Yangtze finless porpoise, the last one was added in the spectrum diagram.

The recording of the noise from a platform, rather than any of the two recordings of the noise from vessels, was chosen for this comparison on account of two reasons. One was the nearest distance from the noise source, which guaranteed that the measured data can present the nature of the noise source better; the other was the higher inferred SL. If the higher noise has impacts on the porpoise, the whole dredging system will impact it; on the contrary, if the higher noise has little possibility of interfering with the porpoise, the lower noise and further the whole system will not have impacts on the finless porpoise.

The noise measured in the southern part of Poyang Lake was assumed to be mainly generated by the nature since there was no dredging activity there. Although the ambient noise in the northern part of the lake may be a little different with the one measure in the southern part due to different geometrical, biological and artificial conditions, compared with the intense noise generated by dredging, the difference can be ignored.

2.5.5 Simulation of Acoustic Environment of Poyang Lake

The noise in Poyang Lake was simulated two dimensionally based on the results of Erbe's experiment (2000) that the SPL of noise varies little in the depth from 0 to 20m ,A computer program based on VB and ArcEngine was developed for the simulation of the noise all over the lake [the interface of the program is shown in Appendix 1]. The simulation consisted of two steps:

1) Computing sound attenuation. For each pixel, the noise impact from every noise source (including dredging platforms and moving vessels) was estimated using the sound propagation model. The distance used in this model was computed between the center of the pixel and the position of the infrastructure. The input frequency of the sound was the geometric mean of the lowest and highest frequency of a bandwidth, because the developed computer program was only available for computing of single frequency. For example, the frequency used for the simulation of the noise map of the narrow bandwidth is 38.34 kHz ($\sqrt{10kHz \times 147kHz}$).

2) Superposition of sound. After calculation the impacts from every noise source, the superposition principle of the decibels was used to calculate the SPL at each pixel. Before the

superposition of the impacts from every vessel, they should firstly be superposed with the ambient noise of the lake. After traversing every pixel in the map of the lake, a simulated noise map can be drawn.

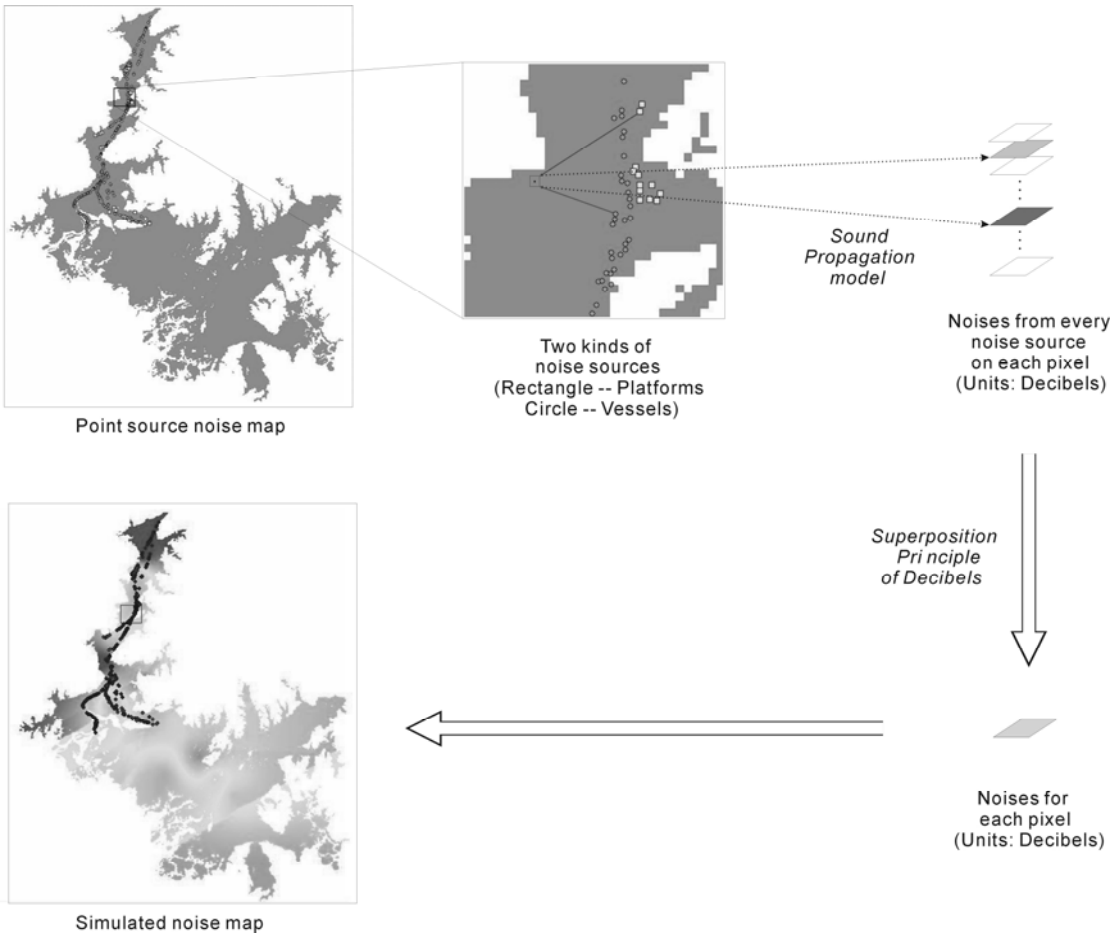

Fig. 13 -- Simulation of noise map

3. Results

3.1 Recorded SPL

Fig. 14 shows the recorded SPL for two bandwidths at sample points (the recording of the field work is shown in Appendix 2). The SPL in the north was higher than the south for both bandwidths, with a cluster of high SPL northwest of sand hill. The high SPL in the north appeared to be discrete instead of continuous, because high SPL occurred adjacent to low. The SPL in the south did not vary as much as in the north and the lowest SPL of both bandwidths existed in the southeast corner of the lake.

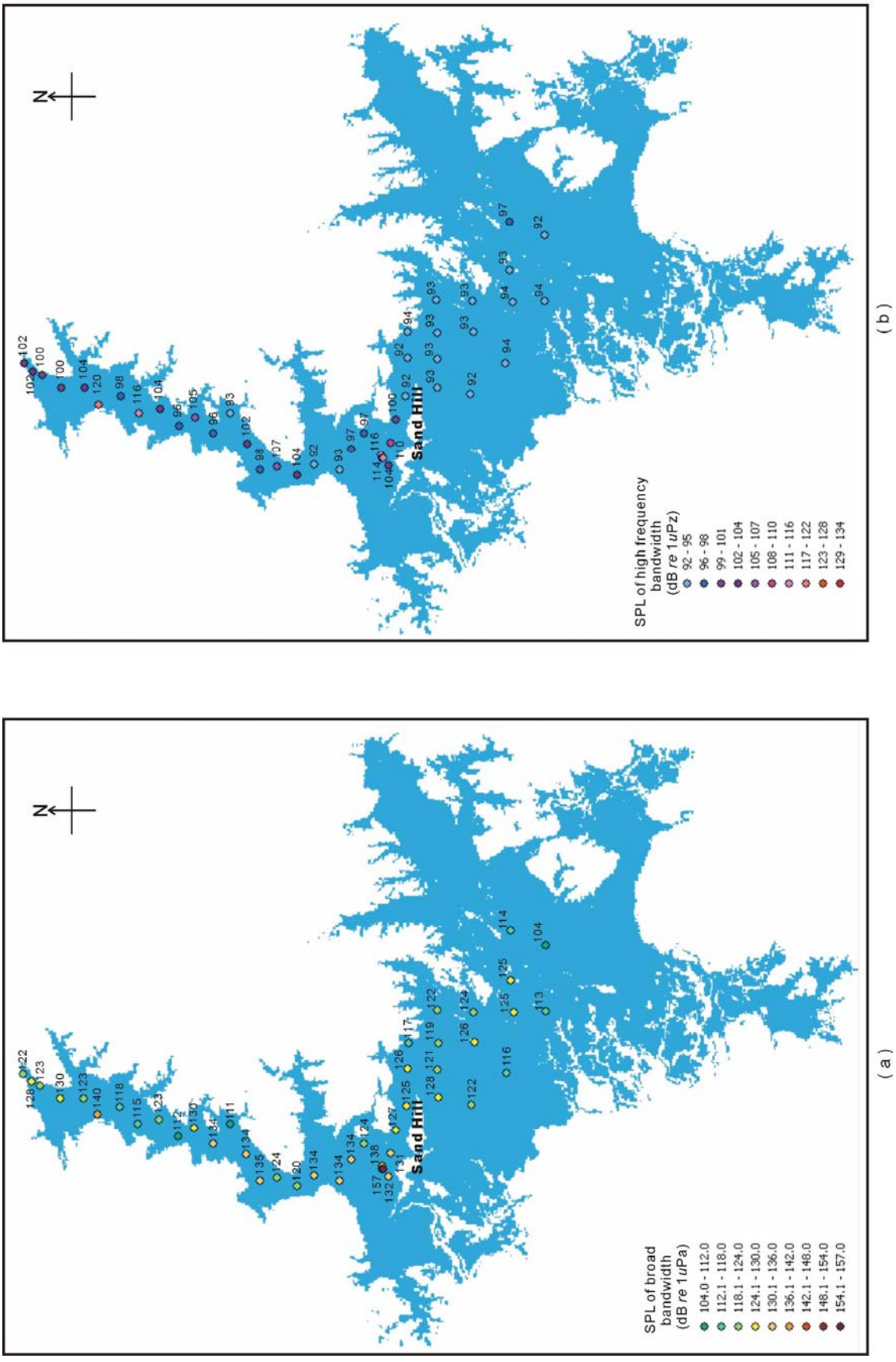

Fig. 14 -- SPL recorded in October 2007 at 42 points in Poyang Lake for (a) broad (0.01 - 147 kHZ) and (b) narrow high frequency (10 - 147 kHz) bandwidth.

The fact that the highest and lowest SPL of both bandwidths coincided does not imply correlation between the SPL of these bandwidths, the correlation coefficient between which was less than 0.5 (0.498). There were some examples where high broad bandwidth SPL coincided with low narrow bandwidth SPL, and vice versa. For instance, broad bandwidth SPL of 134 dB at two points at the bottom of the northern part corresponded to high frequency SPL of only 92 and 93 dB. Moreover, the SPL of broad bandwidth in the southern part of the lake decreased from middle to northeast and southwest gradually, while the SPL in the other bandwidth remained around 93 dB in the whole southern part except one point in the very east.

3.2 Spectrum Diagram of Different Sounds

The recorded noise spectrum diagram presented in Figure 15 reveals that the intensity was higher in the low than in the higher frequency range both for the ambient noise and the noise around the platforms. The figure further shows that the noise levels recorded around the dredging platform were much higher than the ambient noise. Within the peak of the frequency range used for echolocation by the finless porpoise (from 87 kHz to 145 kHz), the amplitude of the ambient noise was much lower than that generated by the porpoise, whereas the intensity of the noise generated from dredging platform reaches as high as the level used by the finless porpoise.

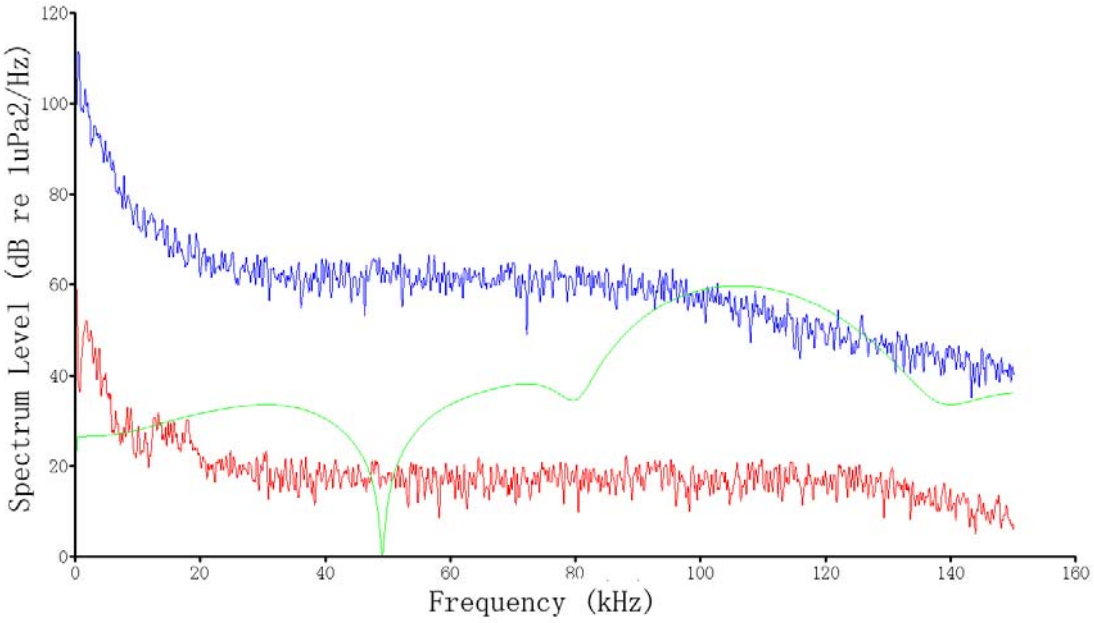

Fig. 15 -- Comparison of spectra of platform, ambient noise and sound used by finless porpoise (blue - noise at dredging site; red - ambient noise; green - sound used by finless porpoise).

3.3 Extracted Point Maps of Platforms and Vessels

The ASTER image of August 2000, taken before the introduction of dredging, revealed few vessels in the Lake [Fig 16 (a)], apart from a few small and hardly visible objects which most likely correspond to small fishing boats. The sum of working platforms and moving vessels in 2005 was 311 and it increased to 367 in 2006 [Tab. 4]. However, the estimated total number of all infrastructures remained the same (474).

Tab. 4 -- Number of platfoorms, moving vessels and other infrastructures in various years estimated from ASTER imagery

YEAR	No. OF DREDGING PLATFORMS	No. OF MOBILE VESSELS	No. OF OTHERS INFRASTRUCTURES
2000	0	0	0
2005	67	244	163
2006	79	288	107

From the comparison between Fig. 16 (b) and Fig. 16 (c), it is clear that the working infrastructures increased in the lower part of the whole dredging area, due to the increase of the dredging platforms north of sand hill. The dredging platforms in that part dispersed. Previous (2005) dredging activity near Hukou (at the top of the image) was not visible in 2006.

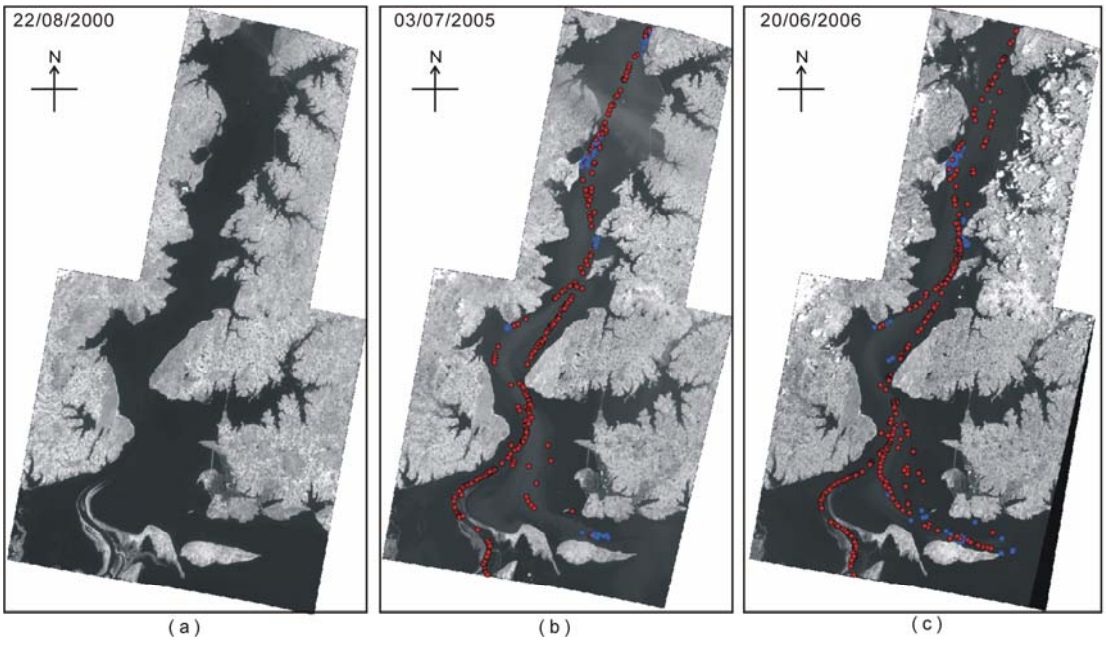

Fig. 16 -- Distribution of dredging platforms and mobile vessels according to ASTER imagery of 2000, 2005, 2006 (blue square - dreding platform; red circle - mobile vessel).

3.4 Noise Maps

3.4.1 Noise Maps of Broad Bandwidth

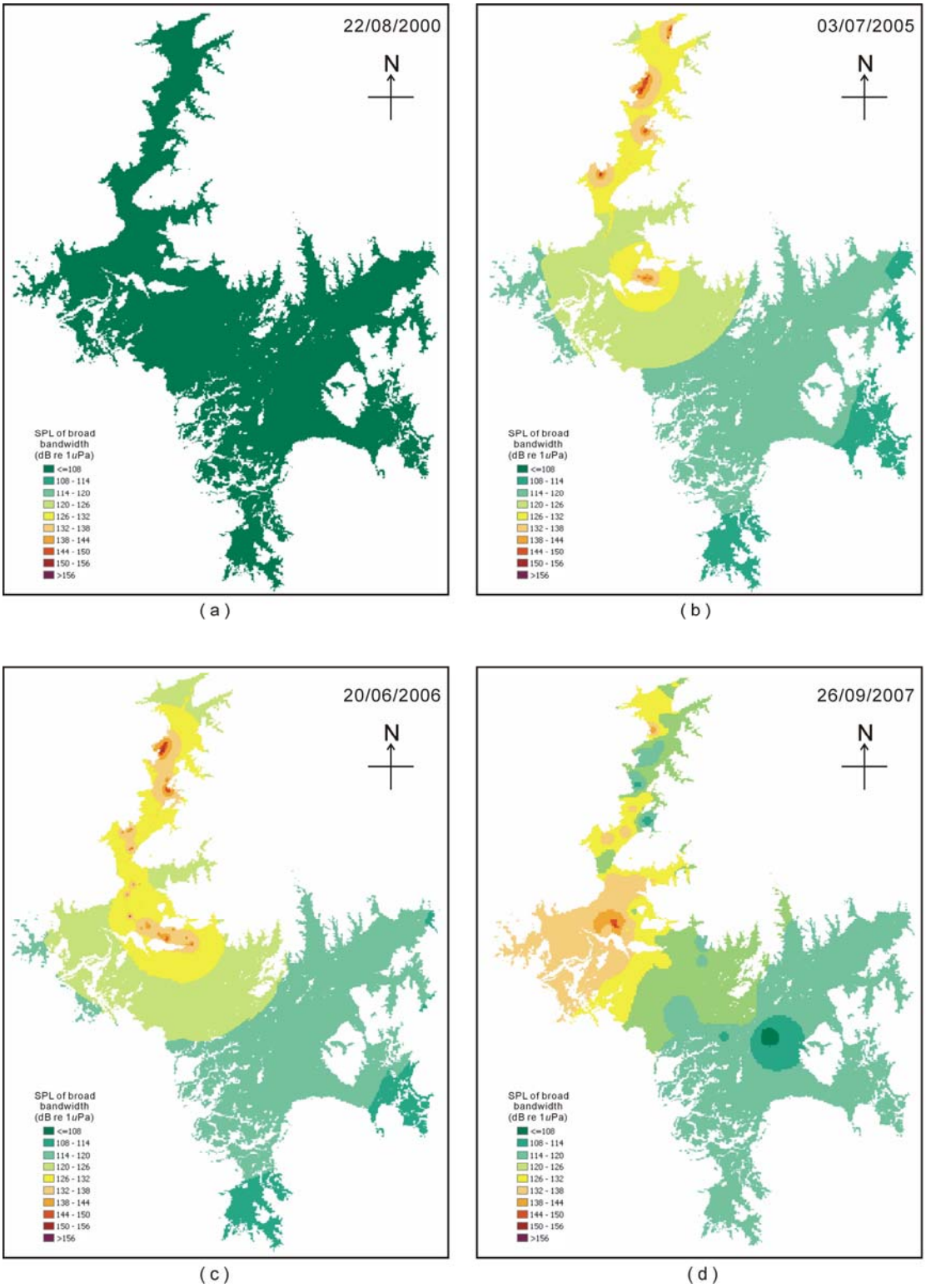

Fig. 17 -- Broad bandwidth noise maps based on vessel locations derived from ASTER imagery in (a) 2000 (b) 2005 (c) 2006 and (d) noise map derived from interpolation of noise levels recorded in situ in Oct. 2007

An ambient noise map was drawn for 2000 because dredging was absent at that time. The lowest SPL for each bandwidth recorded in 2007 in the southern part of the lake was taken to represent the ambient noise without dredging. The SPL maps of 2005 and 2006 were generated using the locations of working infrastructures derived from ASTER images and their inferred SL based on the measurements in 2007. A noise map for October 2007 was generated through interpolation of the SPL recorded at the sample points, using the Inverse Distance Weighting (IDW) method. The SPL was classified in the maps with intervals of 6 dB re 1 μPa. A 6 dB difference in SPL corresponds to a twofold difference in noise intensity, because an algorithm was used to calculate SPL. At high frequency some frequency classes were 3 dB wide.

Generally, in the four simulated noise maps in the broad bandwidth [Fig. 17], the SPL rose from 104 dB (the ambient noise in 2000) to almost no less than 111 dB after 2005, and the highest SPL of the noise reached above 150 dB. At least from 2005, almost the whole northern part of the lake was occupied by the noise higher than 120 dB. The SPL decreased gradually from the highest level at some points in the northern part of the lake to the lowest in the south. In the simulated maps 2005 and 2006, the SPL decreased along the radial direction of circles, but not in 2007. Furthermore, from 2005 to 2007, extent of the noise of high SPL was expanding and spreading from north to south.

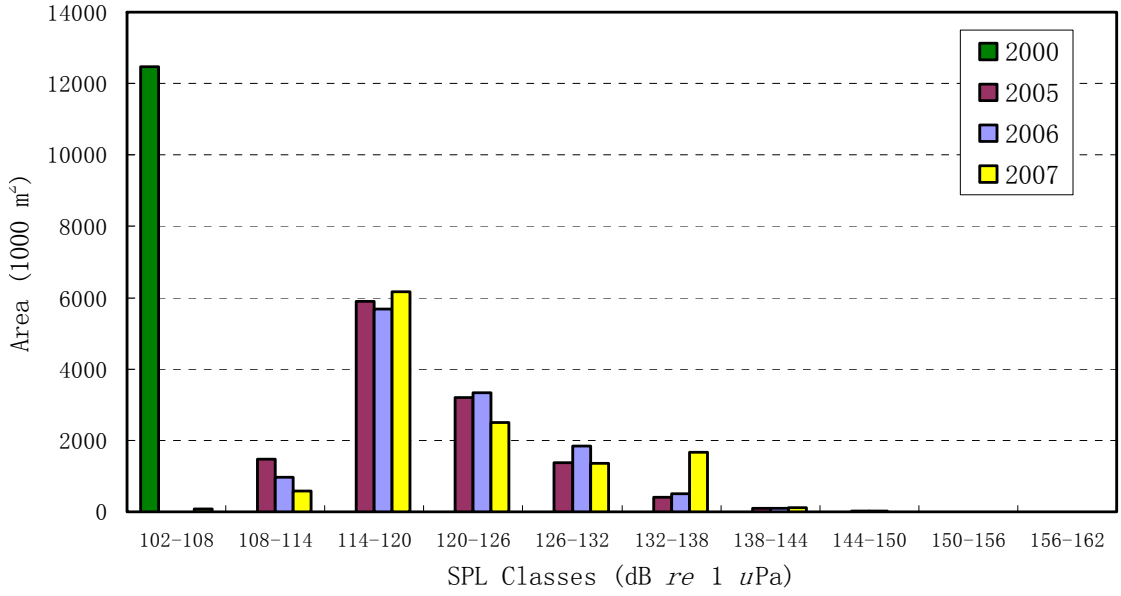

Fig. 18 -- Area exposed to various SPL classes of broad bandwidth (0.01 - 147 kHz) in 2000, 2005, 2006 and 2007.

Tab. 5 -- Area exposed to less and more than 120 dB SPL in 2000, 2005, 2006 and 2007

Year	SPL	
	< 120 dB (km^2)	> = 120 dB
2000	12.5	0.0
2005	7.4	5.1
2006	6.7	5.8
2007	6.8	5.6

Fig. 18 compares the area exposed to various SPL classes. The whole Poyang Lake in 2000 was in the range of 102~108 dB and the noise level increased afterwards. The range of the main SPL of the noise in Poyang Lake shifted from 108 ~132 dB in 2005 to 114 ~ 138 dB in 2007. It also shows the reduction of the areas of low SPL but increase of the area of high SPL. From 2005 to 2006, the areas decreased in the ranges below 120 dB and increased in the ranges up 120 dB. Although the situation was a little different in 2007, there was an obvious increase in the range from 132 dB to 138 dB. From Tab. 5, it can be seen that the areas with SPL higher than 120 dB increased from 5.1 km^2 in 2005 to 5.8 km^2 and 5.6 km^2 in 2006 and in 2007 respectively, area shown by colors from light green to dark red in the noise maps.

3.4.2 Noise Maps of High Frequency Bandwidth

Areas with SPL 3 dB higher than the ambient noise (92 dB) was considered as place where the acoustic environment was unchanged in this frequency range. As shown in Fig. 20, the SPL of this frequency range remained unchanged in most part of the lake, especially in the northern part of the lake. In the simulated noise maps in 2005 and 2006, the extent of changed acoustic environment was quite limited, less than 1.3 km from the center. However, from the interpolated map in 2007, the acoustic environment has changed a lot in the northern part of the lake, with the exception of three points. The highest SPL from 2005 to 2007 were 116.5 dB, 114.9 dB and 125.8 dB respectively.

Fig. 19 shows the areas of changed and unchanged range in 2000, 2005, 2006 and 2007. The area increased slowly from 2000 to 2006 with an increment of 0.11 km^2 from 2000 to 2005 and 0.05 km^2 from 2005 to 2006, but there was a jump from 2006 to 2007. During the one year duration; the increment of the area of changed acoustic environment was about 3.87 km^2, which makes the total changed areas nearly one third of the whole lake.

Fig. 19 -- Area exposed to various SPL class of narrow bandwidth (10 - 147 kHz) in 2000, 2005, 2006 and 2007.

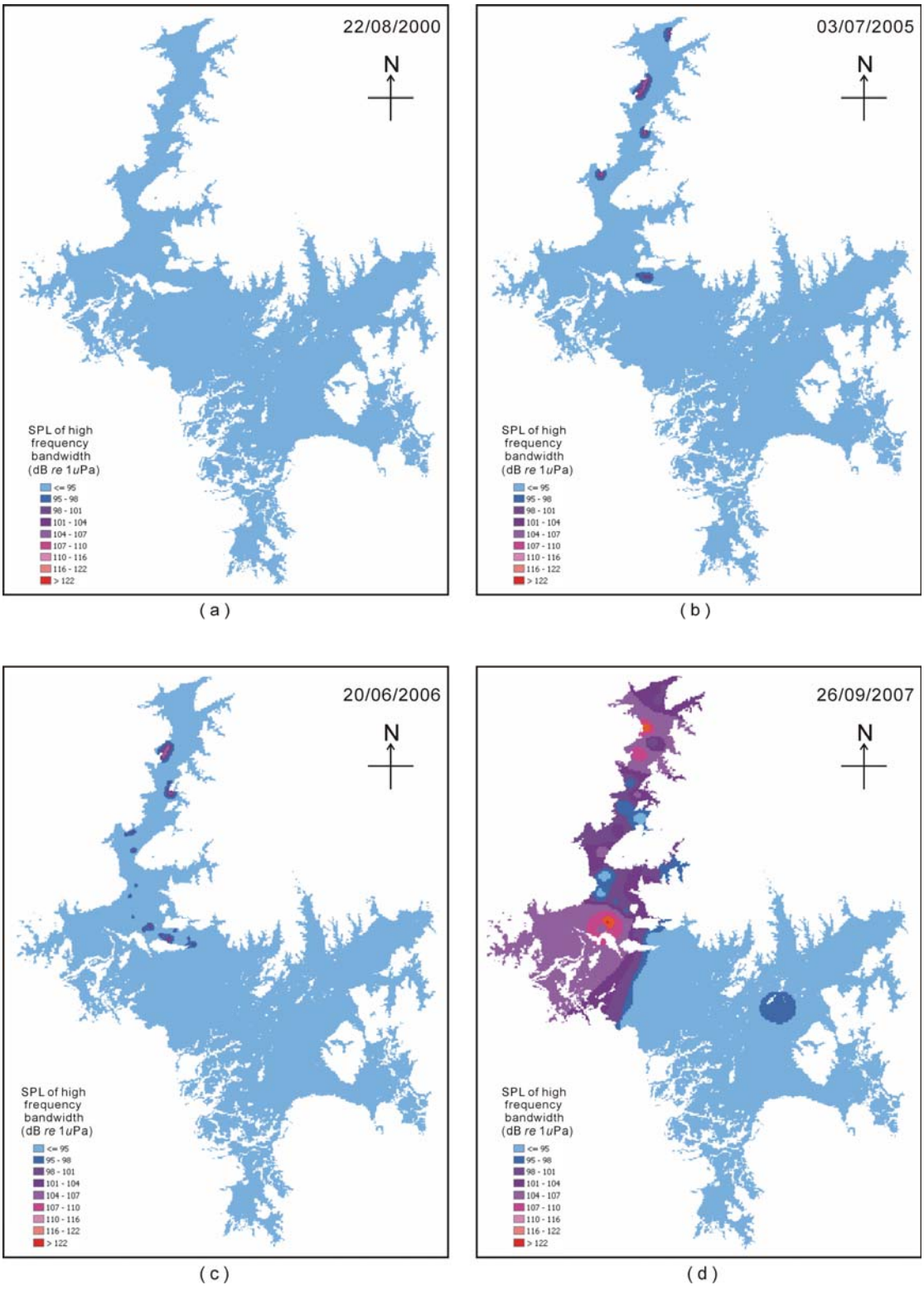

Fig. 20 -- Simulated noise maps of high frequency range. (a) ambient noise map of the lake; (b), (c) simulated noise maps with satellite derived vessel location; (d) interpolated noise map with sample values.

4. Discussion

4.1 Noise from Dredging Infrastructures

In this research, the noises generated by dredging platforms and moving vessels were measured and predicted for broad and narrow bandwidths. The in situ measurement by hydrophone shows that dredging platform generated noise 70 dB (broad bandwidth) and 40 dB (narrow bandwidth) above the ambient noise of the lake. Broad bandwidth noise generated by moving vessels was 50 dB above ambient level, but we failed to detect increased noise levels in the narrow high frequency range. There are two possibilities for the equal SPL between the moving vessels and the ambient noise. It could be that the high frequency noise generated by the moving vessels was not intense enough to change the acoustic environment. It could also be that the high level noise was underestimated as it may have attenuated before reaching the hydrophone. This is a realistic possibility as noise attenuation increases sharply with frequency.

How reliable was the measurement of noise? Did the method impose any limitations? The SPL generated by a platform was measured under the assumption that a cluster of platform and vessels was composed of a single dredging platform and five vessels. In reality, cluster size varied, for example it was frequent to encountered two or more platforms tied together with more or less vessels. For the reasons that 1) ASTER is incapable of telling the number of platforms in one cluster; 2) there is only one platform in a cluster in most cases; 3) it differed much between the SL of dredging platforms and noise from moving vessels, the collected noise sample can still represent the noise from the cluster of dredging platform. Secondly, the recording of the moving vessels was carried out on a static boat so that the distance between the hydrophone and the moving vessels was changing, thereby reducing the accuracy of the inferred SL of it. More accurate measurements can be done if it is allowed to land on the vessels and record the noise from them so as to keep a consistent distance.

4.2 Dredging Infrastructure Detection from Imagery

This research successfully applied stereo pairs of ASTER images to distinguish dredging platforms, mobile vessels and immobile infrastructures. Making this distinction was required as these three categories differ in the noise they produce. The need for this was realized during field work, when it was observed that the dredging platforms and some of the vessels remained immobile in the middle of the lake. As immobile infrastructures do not generate noise, they must be separated from mobile ones. ASTER was the only of the easy-to-obtain satellite imagery which has a stereo pair of near-infrared bands allowing distinction from moving vessels and immobile infrastructures. ASTER imagery further allowed distinguishing larger dredging platforms from smaller sized infrastructures.

Although technically ASTER imagery allowed distinguishing the three categories of dredging infrastructures, there are some limitations of it. The near-infrared band of the stereo pair is not as good as the middle infrared bands in distinguishing vessels from turbid water (Wu, De Leeuw et al. Submitted). The whole lake needed to be divided into several parts according to the reflectance of the water before the classification because in some areas the reflectance of the vessels was the same as the reflectance of the turbid water in other areas. The poor availability of ASTER imagery limited its use for prediction of noise (only three cloud free images were available). The lack of ASTER imagery of the rainy season in 2007 limited the possibility to compare a remote sensing based noise map with the noise levels recorded in the field. However, ASTER was in summary the most suitable and available satellite imagery to derive information on the distribution of noise generating dredging infrastructure covering the period 2000 till 2007.

The working platforms were separated from other infrastructures under an area-dependent criterion. There were some “false platforms” composed of tied-up static vessels classified as working platform due to their big size. The “false platforms” were deleted during the final visual check depending on their surroundings. Fig. 21 shows an example in 2005. These two clusters of vessels were big and static, which satisfy the character of working platform. But judging by their surroundings that there was neither static vessel in the near water, nor other dredging platform around, and being located just in the main channel, they were most likely to be clusters of not working vessels rather than working platforms. Inevitably not all of those “false platforms” could be found out during the check. There were also some vessels missing from the extraction, because their reflectance was too low to be distinguished from the turbid water. Comparing the result of the semi-auto classification with visual examination of the image in that year, the percentage of the number of missing vessels and misclassified ones to the total number of infrastructures was less than 3%, so the result of the extracted dredging infrastructures was considered reliable.

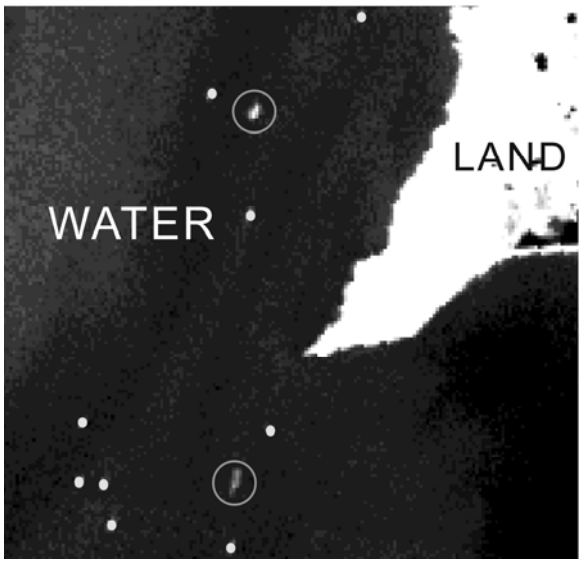

Fig. 21 -- Example for "false platform". Vessels in hollow circles are static and their sizes are big; small solid circle are moving vessels.

Compared with the number of infrastructures in August 2005 counted by Wu from Landsat TM imagery (Wu, de Leeuw et al. 2007), the estimated number of all infrastructures from ASTER imagery was about 90 more. The difference might due to the higher resolution of ASTER images. As shown in Fig. 22, the two clusters of dredging platforms in the white circle at the top left might be counted as one in the Landsat TM image because the space between these clusters was small and might not be clear enough to be recognized in the TM imagery. The three immobile vessels in the other white circle is another example.

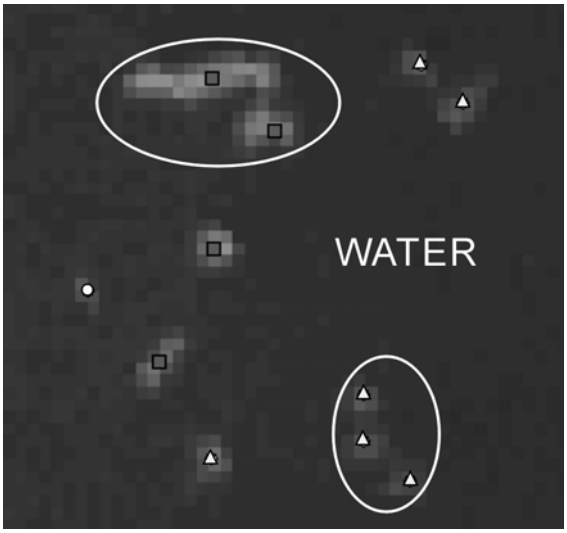

Fig. 22 -- An example in ASTER image in 2005 (rectangle - dredging platform; circle - mobile vessel; triangle - immobile vessel). Note that pixels in a white circle might be estimated as one infrastructure in Landsat TM.

4.3 Noise Propagation Model

The propagation model of noise was built using models derived from literature. The model took into account the two main causes of sound pressure loss, the geometrical spreading loss and the water absorption loss. Before this research, studies of sound propagation of` various bandwidths in different underwater conditions, such as low frequency sound in oceans (Vador 2000; Vador 2001; Vador 2005; Vador 2006), sound loss caused by effects from the sea surface (Schulkin 1968; Schulkin 1969; Zhou, Zhang et al. 2007) and from the internal waves (Yang 2006; Katsnel'son, Badiey et al. 2007) were carried out. The propagation model chosen in this study depended on the real situation of Poyang Lake. The geometrical spreading loss and the water absorption loss in the used model is suitable for shallow water less than 10m and both sound frequency range of broad bandwidth and narrow bandwidth of high frequency.

But values of some parameters used in the model can be improved:

- For temperature, the average values pertaining for the rainy season of that year could be used if available, because the simulated maps represent the situation of the rainy season of one year.

- The distance used in the model was the shortest possible distance between two points. In reality, the straight line joining two points may be blocked by obstacles and the sound has to go across the obstacle in order to reach the target point. In other words, the distance should use the length of the path between the noise source and the target point. This can explain the reason why at some points behind a hill or in a corner recorded SPL was low, but the simulated one was high.

- A reformative version of the computer program will increase the accuracy of the simulated maps by calculating the sound absorption depending on different frequencies. The spectrum of the noise of each noise level will be used as the input, and the program will compute the water absorption loss at every frequency .

4.4 Change Detection of Acoustic Environment

4.4.1 Simulated and Interpolated Noise Maps

In the simulated maps of 2005 and 2006, the SPL of noise diffused approximately in circles. Overlaying the simulated noise maps with the locations of noises sources (platforms and moving vessels), it can be found that the center of the circles are the position of dredging platforms, indicating that the main influence on the acoustic environment in both bandwidths come from the dredging platforms rather than moving vessels, but the reasons are different in each frequency range. In the broad bandwidth (0.01~147 kHz), the SL of dredging platform is nearly 20 dB higher than the moving vessels, so the influence of the moving vessels can be masked by dredging platforms within a range of them. Then in the high frequency range (10~147 kHz), the mobile vessels are considered to have no impacts in this range, meaning that all the influence in this bandwidth come from dredging platforms.

The simulated maps based on the satellite image captured at one moment can still represent the situation of the dynamic acoustic environment in that season, because: 1) according to the simulated noise maps, the great impacts on change of the acoustic environment in both broad and narrow bandwidth come from the noise from dredging platforms rather than moving vessels; 2) for the dredging platforms, their locations are constrained in dredging areas by the government within every season and they remain immobile within a time period during dredging activity; 3) the aims of generating the simulated maps are detecting the change of the acoustic environment and its impacts on the Yangtze finless porpoise, so that the change of several platforms will not cause a fundamental change of the acoustic environment compared with the total number of dredging platforms and the change of it annually. Based on information obtained from processing the ASTER images of 2005 and 2006, the number of dredging platforms increased from 67 to 78. Since there was a proportion between the number of dredging platforms and all vessels, (0.141 and 0.164 in both 2005 and 2006 respectively) and there was a dramatic increase of the number of vessels from 2000 to 2005 (Wu, de Leeuw et al. 2007), it can be estimated that the increase of

dredging platforms was also remarkable, which would arouse notable change of the acoustic environment.

The interpolated maps in 2007 are different with the simulated maps in 2005 and 2006 in the shape and extent of noise impact, especially in the high frequency range. The inconsistence of the simulated noise maps in 2005 and 2006 with the interpolated map in 2007 might be because of the reason that the interpolation method did not match the sound propagation principle very well. Within the domain of sample points, the accuracy is relatively higher because of the restrictions from the value of the sample points around, but in the extrapolated range, for the reason that the decay rate of the SPL of the noise is much slower in the interpolation method than the real situation, particularly in the high frequency range, the extent of impacted range appears larger than the actual situation. Furthermore, the interpolated maps took the anomaly transmission loss (i.e. scattering loss) into account, which were not included in the sound propagation model for the simulation of the noise maps, so the shape of the interpolated map is not as regular as the simulated maps but more closer to the situation in reality.

Generally, the simulated maps can represent the acoustic environment of the rainy season of the corresponding year in a large scale whereas the interpolated maps in 2007 enlarge the extent and intensity of the noise but good at reflecting details of the acoustic environment in the interpolated range.

4.4.2 Change Detection

Our results demonstrated a marked change of the acoustic environment in the northern part of Poyang Lake as a result of intensive dredging activities there. Together with the increment of the working infrastructures, the area of high SPL in both bandwidths increased. The change was different in various bandwidths because the energy of the generated noise from dredging mainly concentrated in the low frequency range.

In the broad bandwidth (0.01~147 kHz), the SPL of noise over the whole lake rose to a higher level (7 dB higher) than the ambient noise from at least 2005, which means that even at the quietest place, the intensity of the noise was more than twice high as the original noise. From 2005 to 2007, the points with highest SPL changed with the location of dredging platforms. In general there was a trend of increasing intensity of noise extending the area of high SPL from north to south.

In the narrow bandwidth (10~147 kHz), considering that the interpolated map in 2007 enlarged the extent of impacts, the change detection should mainly be based on the maps in 2005 and 2006, but refer to the measured data in 2007. In sum, the SPL remains unchanged at more than 98% of the lake, except for some points in the northern part of the lake. The same as in the broad bandwidth, the range of the changed SPL depended on the location of dredging platforms, but the extent of the influence is quite limited. However, the total area of the changed SPL was increasing from 2005. Referring to sample points in 2007 [Fig. 14 (b)], there were some relatively high SPL of high

frequency noise near Hukou. It might be caused by the wind or from noise from transportation vehicles from the bridge there.

4.5 Possible Impacts on Porpoise

Our research revealed overlap between the peak acoustic range used by finless porpoise and the noise generated by dredging platform. Although the distance traveled by the signal varied according to different relative location of the targets, the intensity of the returned signal is surely lower than the emitted signal after spreading in the water, thus lower than the intensity of noise from dredging platform in that frequency range. Fletcher's principle stated that a signal will be masked by noise with equal or higher intensity in the same critical band (Fletcher 1940), indicating that the porpoise can hardly distinguish its signal from the noisy environment. That is to say, within a certain range of the dredging platform, the echolocation of the Yangtze finless porpoise will be impacted.

From the simulated noise maps in high frequency range (including the acoustic range of the porpoise), the range of the change of the SPL was not so wide, which means that the influence of noise with high frequency on the echolocation was not so much in the rainy season, but it might be still important during the dry season when the lake becomes very narrow. Moreover, as have discussed, it is also very dangerous for the porpoise to swim into the small range which may mask they signals for navigation and might kill them accidentally.

Besides impacts on navigation, there are some other potential impacts on the porpoise by noise. It is evident that broad bandwidth noise of more than 120 dB *re* 1 μPa disturbs most marine mammals (Richardson, Greene et al. 1995), the area with SPL higher than 120 dB on the noise maps of broad bandwidth was considered to have disturbance on the Yangtze finless porpoise. From the noise maps, nearly the whole northern part of Poyang Lake was covered by noise louder than 120 dB. Suppose that all the living conditions were the same over the whole Poyang Lake in the rainy season, the porpoise would avoid the area with SPL higher than 120 dB, only living in the main body of the lake. This would isolate the porpoise in Poyang Lake from the subpopulation in the Yangtze, which is biologically harmful to the survival of this species. But in the reality, affected by the distribution of fish and the suitable water depth (Yu, Wang et al. 2005), the distribution of the finless porpoise overlaps with the area where the SPL is higher than 120 dB, although they have to suffer from the high noise intensity. At the same time, it can also be deduced that during the dry season of Poyang Lake, when both the dredging activities and the Yangtze finless porpoise are constrained in the deep area in the northern part of the lake, the hearing of the porpoise might be impaired due to exposure to intense noise for a long period.

4.6 Summary

The innovation of this research is the introduction of RS to localize both static and mobile noise generating sources separately, not only restricted to single noise source, together with the monitoring of the change of the acoustic environment polluted by these noise sources. RS provides a convenient way to map the distribution of all noise sources. Combined with the sound propagation model and the SL of noise sources, the acoustic environment of the whole water area can be mapped. Another advantage of using RS is its ability of recurring historical situation from satellite image. This provides not only a possibility to understand the acoustic environment years ago, but also a convenient way to detect the change of the acoustic environment. The sound propagation model underwater in Poyang Lake was derived based on the studies on underwater noise. The possible impacts on the Yangtze finless porpoise was deducted from the comparison of the sound use by this animal with the structure of noise, and the common responses to a certain noise level of marine mammals. If combined with a historical data with the distribution of the Yangtze finless porpoise, it is better to assess the impacts of the noise on this species.

5. Conclusions and Recommendations

5.1 Conclusions

The objective of this study was to detect the change of the acoustic environment in Poyang Lake based on remote sensing derived localization of dredging infrastructure for assessing the impacts of the noise on the Yangtze finless porpoise. In order to reach this objective, this study explored three specific objectives: 1) to extract location of two dredging infrastructures from satellite image; 2) to detect the change of the acoustic environment; 3) to assess the possible impacts on the finless porpoise of the changes acoustic environment. The specific conclusions inferred from this study are summarized as follows:

- The extraction of the location of dredging infrastructures and the distinguishing of them can be achieved using the ASTER image, because of its unique stereo pair of the 3N and 3B bands of 15m resolution in VNIR subsystem. The near-infrared bands can be used to detect all dredging infrastructures from turbid water. Next, the stereo pair is used to distinguish the working transporting vessels from other infrastructures. Finally, the working platform can be separated from non functional infrastructures based on the size difference, which is feasible because of the high resolution of the VNIR image. However, the limited availability of data is the biggest limitation of ASTER image in this study.

- Based on the ambient noise maps in 2000, simulated noise maps in 2005 and 2006, and the interpolated noise maps in 2007 of both broad and narrow bandwidths, the main impacts on

the acoustic environment came from dredging platforms instead of moving vessels, but the extents of change are different in these two bandwidths. In the broad bandwidth, the acoustic environment over the whole lake has been totally changed from 2000. The highest SPL of noise concentrate in the northern part of the lake, where the dredging activities are, and in most part of it, the SPL is higher than 120 dB *re* 1 μPa. The range of the noise with high intensity is expanding and spreading from north to south. But in the high frequency range, the change is not as much as it is in the broad band width. The range of the changed SPL is quite limited in the northern part of the lake, and the highest SPL is only 30 dB higher than the ambient noise compared with more than 50 dB higher in the broad bandwidth. Therefore, the change of the acoustic environment is mainly in the low frequency range, and the change of it is remarkable, especially in the northern part of Poyang Lake.

- Since there is an overlap between the noise generated by dredging platform and the peak of the sound used by the Yangtze finless porpoise (from 90 kHz to 130 kHz), there should be some impacts from the dredging platform on the echolocation of the finless porpoise. Because the porpoise mainly use the echolocation for navigation and prey, it is reasonable to assume that within in a certain range of dredging platform, the porpoise will be disturbed. But for the reason that the change of the acoustic environment in the high frequency range is quite limited, the range of the disturbance on the echolocation of the Yangtze finless porpoise is not so wide. However, besides the interference with the echolocation, it is also possible that the porpoise will be disturbed by noise in broad bandwidth with SPL higher than 120 dB. Since nearly the whole northern part of Poyang Lake is louder than 120 dB, there is a high potential to harm the porpoise living there. Moreover, in both broad bandwidth and in high frequency range, the situation will be aggravated in the dry season when the porpoise is forced to live near to the sites of dredging activities when the water volume shrinks.

5.2 Recommendations

This study is considered as a preliminary research on modeling the acoustic environment using the remote sensing. And there is no mature model for the sound propagation in the shallow lake water. Moreover, because of some limitations, the sample noise data for dredging platforms and moving vessels is not enough. So, in order to improve the result of the simulated noise maps, 1) experiments should be carried out to build a sound propagation model in Poyang Lake; 2) the number of the noise samples for dredging platform groups should be increased, including the combination of different number of platforms and vessels; 3) the measurement of the noise from moving vessels should be carried out with the hydrophone dragged from the vessel.

The validation of the simulated noise maps should be done if there is an ASTER image around the date of the field work. More ASTER images should be searched after 2007 in order to detect the change of the acoustic environment better, because the findings are only based on the data in 2005, 2006 and 2007, it is not so enough to observe the trend of the change.

This research only brings forward a possibility of impacting the Yangtze finless porpoise by the noise from dredging activities and the noise maps. More studies on the reaction of the Yangtze finless porpoise to noise with different intensity and frequencies should be carried out to assess the real impacts of the noise on this animal. Furthermore, because of the absence of the data on the distribution of the Yangtze finless porpoise, and data on other factors which affect the habitat selection of the Yangtze finless porpoise, it is hard to assess the importance of the noise distribution on its habitat selection and the impacts on the survival of this species. In order to save this species, a project should be carried out on studying all the factors influencing its survival with noise maps being considered a factor.

Meanwhile, steps aimed at preventing a further deterioration of the acoustic environment should be taken. The dredging activities should be constrained to some areas which is not so important for the finless porpoise. Then, the noise generated by the dredging activities should be reduced and limited to frequencies outside the range used by the Yangtze finless porpoise. These measures should be carried out as soon as possible so as to prevent any adverse effect on this animal.

References

Akamatsu, T., D. Wang, et al. (1998). "Echolocation range of captive and free-ranging Baiji (*Lipotes vesillifer*), finless porpoise (*Neophocaena phocaenoides*), and bottlenose dolphin (*Tursiops truncatus*)." Journal of Acoustic Society of America **104**(4): 2511-2516.

Au, W. W. L. (1993). The sonar of dolphins. New York, Springer-Verlag.

Bowlin, J., J. Spiesberger, et al. (1992). Ocean acoustical ray-tracing software RAY. Tech. Rep. WHOI-93-10. Woods Hole, MA, Woods Hole Oceanographic Institution.

Braulik, G. T. (2006). "Status assessment of the Indus River dolphin, Platanista gangetica minor, March-April 2001." Biological Conservation **129**(4): 579-590.

Brekhovskikh, L. and Y. Lysanov (1982). Fundamentals of Ocean Acoustics. Berlin, Heidelberg, New York, Springer-Verlag.

Burgess, D. W. (1993). "Automatic ship detection in satellite multispectral imagery." Photogrammetric Engineering and Remote Sensing **59**: 229-237.

Chen, K., X. Zeng, et al. (2005). Sound Survey. Beijing, Science Press.

Courmontagne, P. (2005). "An improvement of ship wake detection based on the radon tranform." Signal Processing **85**(8): 1634-1654.

Erbe, C. (2002). "Underwater noise of whale-watching boats and potential effects on killer whales (Orcinus orca), based on an acoustic impact model." Marine Mammal Science **18**(2): 394-418.

Erbe, C. and D. M. Farmer (1998). "Masked hearing thresholds of a beluga whale (Delphinapterus leucas) in icebreaker noise." Deep Sea Research Part II: Topical Studies in Oceanography **45**(7): 1373-1388.

Erbe, C. and D. M. Farmer (2000). "A software model to estimate zones of impact on marine mammals around anthropogenic noise." Journal of the Acoustical Society of America **108**(3): 1327-1331.

Erbe, C. and D. M. Farmer (2000). "Zones of impact around icebreakers affecting beluga whales in the Beaufort Sea." Journal of the Acoustical Society of America **108**(3): 1332-1340.

Erbe, C., A. R. King, et al. (1999). "Computer models for masked hearing experiments with beluga whales (Delphinapterus leucas)." Journal of the Acoustical Society of America **105**(5): 2967-2978.

Fletcher, H. (1940). "Auditory patterns." Review of Modern Physics **12**: 47-65.

Gao, A. and K. Zhou (1995). "Geographical variation of external measurements and three subspecies of Neophocaena Phocaenoides in Chinese waters." Acta Theriologica Sinica **15**(2): 81-92.

IUCN (2007). "2007 IUCN Red List of Threatened Species." <www.iucnredlist>. Downloaded on 22 February 2008.

Kastak, D., R. J. Schusterman, et al. (1999). "Underwater temporary threshold shift induced by octave-band noise in three species of pinniped." Journal of the Acoustical Society of America **106**(2): 1142-1148.

Kastelein, R. A., S. van der Heul, et al. (2006). "The influence of underwater data

transmission sounds on the displacement behaviour of captive harbour seals (Phoca vitulina)." Marine Environmental Research **61**(1): 19-39.

Kastelein, R. A., W. C. Verboom, et al. (2005). "The influence of acoustic emissions for underwater data transmission on the behaviour of harbour porpoises (Phocoena phocoena) in a floating pen." Marine Environmental Research **59**(4): 287-307.

Katsnel'son, B. G., M. Badiey, et al. (2007). "Horizontal refraction of sound in shallow water and its experimental observations." Acoustic Physics **53**(3): 313-325.

Li, S. H., K. X. Wang, et al. (2005). "Echolocation signals of the free-ranging Yangtze finless porpoise (Neophocaena phocaenoides asiaeorientialis)." Journal of the Acoustical Society of America **117**(5): 3288-3296.

Ligon, F. K., W. E. Dietrich, et al. (1995). "Downstream ecological effects of dams: a geomorphic perspective." BioScience **45**: 183-192.

Liu, Y., M. Fang, et al. (2003). An Automatic Ship Detection System using ERS SAR images. Proceedings of International Geoscience and Remote Sensing Symposium (IGARSS)'03.

Martin, A. R. and V. M. F da Silva (2004). "Number, seasonal movements, and residency characteristics of river dolphins in an Amazonian floodplain lake system." Canadian Journal of Zoology **82**(8): 1307-1315.

Matthews, J. (2005). "Stereo observation of lakes and coastal zones using ASTER imagery." Remote Sensing of Environment **99**(1-2): 16-30.

McDonnel, M. J. and A. J. Lewis (1978). "Ship detection from Landsat imagery." Photogrammetric Engineering and Remote Sensing **44**: 297-301.

Parsons, C. and S. Dolman (2003). Noise as a problem for cetaceans. Oceans of noise. M. Simmonds, S. Dolman and L. Weilgart, Whale and Dolphin Conservation Society**:** 53-61.

Popov, V. V., A. Y. Supin, et al. (2005). "Evoked-potential audiogram of the Yangtze finless porpoise *Neophocaena phocaenoides asiaeorientalis* (L)." Journal of Acoustic Society of America **117**(5): 2728-2731.

Reeves, R., R. and A. A. Chaudhry (1998). "Status of the Indus River dolphin *Platanista minor*." Oryx **32**(1): 35-44.

Reeves, R., R., B. D. Smith, et al., Eds. (2000). Biology and conservation of freshwater cetaceans in Asia. Occasional Papers of the IUCN Species Survival Commission

Richardson, W. J., C. R. Greene, et al. (1995). Marine Mammals and Noise San Diego, CA, Academic Press.

Rojas-Bracho, L., R. Reeves, R., et al. (2006). "Conservation of the vaquita *Phocoena sinus*." Mammal Review **36**(3): 179-216.

Schulkin, M. (1968). "Surface-Coupled Losses in Surface Sound Channels." Journal of Acoustic Society of America **44**(4): 1152-1154.

Schulkin, M. (1969). "Surface-Coupled Losses in Surface Sound Channel Propagation." Journal of Acoustic Society of America **45**(4): 1054-1055.

Simmonds, M., S. Dolman, et al. (2003). Oceans of noise, Whale and Dolphin Conservation Society.

Smith, B. D., R. K. Sinha, et al. (1994). "Status of Ganges River Dolphines (Platanista gangetica) in the Karnali, Mahakali, Narayani and Sapta Kosi Rivers of Nepal and

India in 1993." Marine Mammal Science **10**(3): 368-375.

Tello, M., C. Lopez-Martinez, et al. (2006). "Automatic vessel monitoring with single and multidimensional SAR images in the wavelet domain." ISPRS Journal of Photogrammetry and Remote Sensing **61**(3-4): 260-278.

Tello, M., C. Lopez-Martinez, et al. (2006). "Automatic vessel monitoring with single and multidimentional SAR images in the wavelet domain." ISPRS Journal of Photogrammetry and Remote Sensing **61**: 260-278.

Tunaley, J. K. E. (2004). Algorithms for ship detection and tracking using satellite imagery. Proceedings of International Geoscience and Remote Sensing Symposium (IGARSS)'04.

Vador, R. A. (2000). "Low-Frequency Sound Absorption and Attenuation in Marine Medium." Acoustic Physics **46**(5): 544-550.

Vador, R. A. (2001). "Long-Range Sound Propagation in the Central Region of the Baltic Sea." Acoustic Physics **47**(2): 150-159.

Vador, R. A. (2005). "Long-Range Sound Propagation in the Northeastern Atlantic." Acoustic Physics **51**(6): 629-637.

Vador, R. A. (2006). "Acoustic Propagation in the Surface Sound Channel." Acoustic Physics **52**(1): 6-16.

Wang, K. X., D. Wang, et al. (2006). "Range-wide Yangtze freshwater dolphin expedition: The last chance to see Baiji?" Environmental Science and Pollution Research **13**(6): 418-424.

Wang, P. (1992). "On the taxonomy of the finless porpoise in China." Fisheries Science **11**(6): 10-14.

Wu, G., J. De Leeuw, et al. (Submitted). Performance analysis of Landsat TM bands for dredging ship detection in turbid water of the northern Poyang Lake, China.

Wu, G., J. de Leeuw, et al. (2007). "Concurrent monitoring of vessels and water turbidity enhances the strength of evidence in remotely sensed dredging impact assessment." Water Research **41**(15): 3271-3280.

Wuersig, B. and C. R. Greene (2002). "Underwater sounds near a fuel receiving facility in western Hong Kong: relevance to dolphins." Marine Environmental Research **54**(2): 129-145.

Wursig, B. and C. R. Greene (2002). "Underwater sounds near a fuel receiving facility in western Hong Kong: relevance to dolphins." Marine Environmental Research **54**(2): 129-145.

Xiao, W. and X. F. Zhang (2002). "Distribution and population size of Yangtze finless porpoise in Poyang Lake and its branches." ACTA THERIOLOGICA SINICA **22**(1): 7-14.

Yang, J., W. Xiao, et al. (2000). "Studies on the distribution, population size and the active regularity of *Lipotes Vexillifer* and *Neophocaena Phocaenoides* in Dongting Lake and Poyang Lake." Resources and Environment in the Yangtze Basin **9**(4): 444-450.

Yang, T. C. (2006). "Measurements of temporal coherence of sound transmissions through shallow water." Journal of Acoustic Society of America **120**(5): 2595-2614.

Yu, D., J. Wang, et al. (2005). "Primary Analysis on Habitat Selection of Yangtze Finless Porpoise in Spring in the Section Between Hukou and Digang." ACTA

THERIOLOGICA SINICA **25**(3): 302-306.

Zhang, X. F., R. Liu, et al. (1993). "The population of Finless Porpoise in the middle and lower reaches of Yangtze River." ACTA THERIOLOGICA SINICA **13**(4): 260-270.

Zhao, X. (2007). Range-wide Expedition Report. Yangtze Freshwater Dolphin Expedition 2006**:** 1-26.

Zhong, Y. and S. Chen (2005). "Impact of dredging on fish in Poyang Lake." Jiangxi Fish. Sci. Technol **1**: 15-18.

Zhou, J., X. Zhang, et al. (2007). "Sea surface effect on shallow-water reverberation." Journal of Acoustic Society of America **121**(1): 98-107.

Appendices

Appendix 1 -- Interface of the computer program for the simulation of noise maps

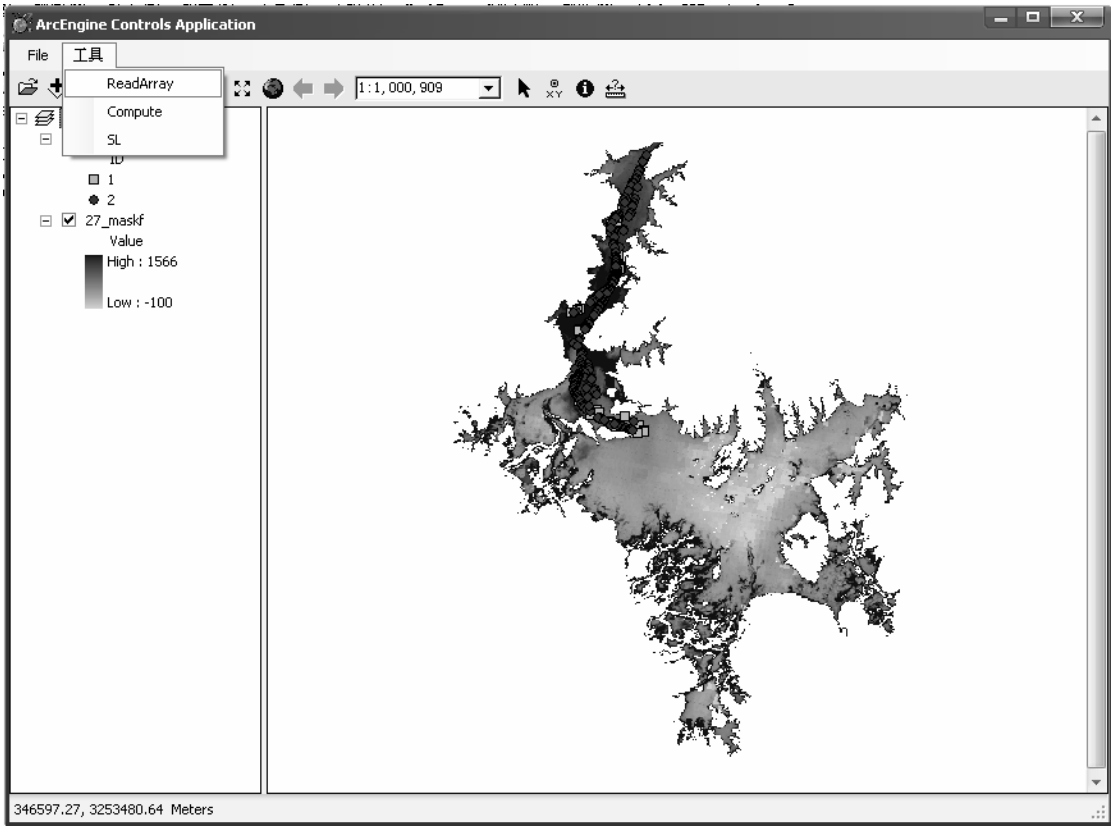

Appendix 2 -- Recordings of the sample points in the field

GPS_ID	Date	Latitude	Longitude	Thru_dB	Hp_dB
640	25-09-2007	29.75196667	116.21473333	122.0	102
641	25-09-2007	29.74056667	116.20210000	128.0	102
643	25-09-2007	29.72808333	116.19618333	123.0	100
644	25-09-2007	29.70148333	116.17608333	130.0	100
645	25-09-2007	29.66873333	116.17670000	123.0	104
646	25-09-2007	29.64958333	116.15111667	140.0	120
647	25-09-2007	29.61960000	116.16410000	118.0	98
648	25-09-2007	29.59435000	116.13781667	115.0	116
649	25-09-2007	29.56498333	116.14398333	123.0	104
650	25-09-2007	29.53886667	116.11700000	112.0	96
651	25-09-2007	29.51631667	116.13130000	130.0	105
652	25-09-2007	29.49116667	116.10651667	134.0	96
653	25-09-2007	29.46796667	116.13801667	111.0	93
654	25-09-2007	29.44478333	116.09045000	134.0	102

655	25-09-2007	29.42600000	116.04820000	135.0	98
656	25-09-2007	29.40271667	116.05338333	124.0	107
657	25-09-2007	29.37475000	116.04000000	120.0	104
658	26-09-2007	29.35183333	116.05753333	134.0	92
659	26-09-2007	29.31641667	116.05008333	134.0	93
661	26-09-2007	29.30085000	116.08380000	134.0	97
662	26-09-2007	29.28330000	116.10895000	124.0	97
663	26-09-2007	29.25883333	116.07386667	138.0	116
664	26-09-2007	29.25790000	116.06796667	146.0	134
665	26-09-2007	29.25690000	116.06820000	157.0	114
666	26-09-2007	29.24928333	116.05635000	132.0	104
667	26-09-2007	29.24696667	116.09345000	131.0	110
668	26-09-2007	29.23961667	116.12970000	127.0	100
669	26-09-2007	29.22640000	116.16778333	125.0	92
670	26-09-2007	29.22420000	116.22668333	126.0	92
671	27-09-2007	29.18196667	116.18158333	128.0	93
674	27-09-2007	29.18330000	116.22525000	121.0	93
675	27-09-2007	29.13685000	116.17061667	122.0	92
676	27-09-2007	29.13343333	116.26835000	126.0	93
677	27-09-2007	29.08953333	116.22076667	116.0	94
678	27-09-2007	29.07948333	116.31548333	125.0	94
679	27-09-2007	29.03590000	116.31781667	113.0	94
680	27-09-2007	29.03576667	116.42016667	104.0	92
681	27-09-2007	29.08465000	116.44270000	114.0	97
682	27-09-2007	29.08330000	116.36490000	125.0	93
683	27-09-2007	29.13480000	116.31603333	124.0	93
684	27-09-2007	29.18420000	116.31806667	122.0	93
685	27-09-2007	29.18275000	116.26643333	119.0	93
686	27-09-2007	29.22411667	116.26668333	117.0	94